N72-32938

NASA CONTRACTOR REPORT

NASA CR-2112

NASA CR-2112

TRANSPORT PROPERTIES OF GASES AND BINARY LIQUIDS NEAR THE CRITICAL POINT

by J. V. Sengers

Prepared by
UNIVERSITY OF MARYLAND
College Park, Md. 20742

for Lewis Research Center

NATIONAL AERONAUTICS AND SPACE ADMINISTRATION • WASHINGTON, D. C. • SEPTEMBER 1972

1. Report No.
NASA CR-2112

2. Government Accession No.

3. Recipient's Catalog No.

4. Title and Subtitle
TRANSPORT PROPERTIES OF GASES AND BINARY LIQUIDS NEAR THE CRITICAL POINT

5. Report Date
September 1972

6. Performing Organization Code

7. Author(s)
J. V. Sengers

8. Performing Organization Report No.
None

9. Performing Organization Name and Address
University of Maryland
College Park, Maryland 20742

10. Work Unit No.

11. Contract or Grant No.
NGR 21-002-344

12. Sponsoring Agency Name and Address
National Aeronautics and Space Administration
Washington, D.C. 20546

13. Type of Report and Period Covered
Contractor Report

14. Sponsoring Agency Code

15. Supplementary Notes
Project Manager, R. J. Simoneau, Physical Sciences Division, NASA Lewis Research Center, Cleveland, Ohio

16. Abstract

A status report is presented on the anomalies observed in the behavior of transport properties near the critical point of gases and binary liquids. The shear viscosity exhibits a weak singularity near the critical point. An analysis is made of the experimental data for those transport properties, thermal conductivity and thermal diffusivity near the gas-liquid critical point and binary diffusion coefficient near the critical mixing point, that determine the critical slowing down of the thermodynamic fluctuations in the order parameter. The asymptotic behavior of the thermal conductivity appears to be closely related to the asymptotic behavior of the correlation length. The experimental data for the thermal conductivity and diffusivity are shown to be in substantial agreement with current theoretical predictions.

17. Key Words (Suggested by Author(s))
Transport properties, Dense gases, Binary liquids, Critical point, Thermal conductivity, Viscosity, Thermodynamics, Scaling parameters, Diffusivity

18. Distribution Statement
Unclassified - unlimited

19. Security Classif. (of this report)	20. Security Classif. (of this page)	21. No. of Pages	22. Price*
Unclassified	Unclassified	73	$3.00

* For sale by the National Technical Information Service, Springfield, Virginia 22151

FOREWORD

The research described in this report was sponsored by the National Aeronautics and Space Administration under grant NGR 21-002-344 and by the Advance Research Project Agency through the Center for Materials Research at the University of Maryland. Computer time for this project was provided by the Computer Science Center of the University of Maryland.

Professor H. L. Swinney provided his original Rayleigh scattering data for carbon dioxide for this research, and Professor G. F. Allen, Professor D. McIntyre, and Dr. B. Le Neindre made available their experimental data prior to publication.

Page intentionally left blank

TABLE OF CONTENTS

LIST OF TABLES

LIST OF FIGURES

Figure | Page

SECTION I

INTRODUCTION

Upon approaching a critical point a system will exhibit large thermal fluctuations in the order parameter. The effect is a direct consequence of the divergence of the susceptibility which determines the strength of these fluctuations [L1]. The word "susceptibility" is used here in a generalized sense indicating the derivative of the thermodynamic variable representing the order parameter with respect to its conjugate field. Thus for binary mixtures the susceptibility refers to $(\partial c/\partial\mu)_{T,P}$ where c is the concentration and μ the chemical potential of either component. The corresponding quantity for a one-component gas with density ρ and pressure P is $(\partial\rho/\partial\mu)_T$ or the isothermal compressibility $K_T = \rho^{-1}(\partial\rho/\partial P)_T$.

Near the critical point the fluctuations in the order parameter decay slowly in time. This process has become known as the phenomenon of critical slowing down of the fluctuations. In a binary liquid mixture the time dependence of the relevant concentration fluctuations with wave vector $\vec{k}$ can be described by a diffusion equation

$$\langle c_k(t)c_{-k}(0)\rangle = \langle|c_k|^2\rangle e^{-Dk^2t} , \tag{1}$$

where D is the binary diffusion coefficient. For a gas it is convenient to separate the density fluctuations into adiabatic pressure fluctuations which propagate with the sound velocity and entropy fluctuations whose intensity is strongly divergent and which decay in a diffusive mode

$$\langle s_k(t)s_{-k}(0)\rangle = \langle|s_k|^2\rangle e^{-\chi k^2t} \tag{2}$$

The thermal diffusivity χ is related to the thermal conductivity coefficient λ and the specific heat at constant pressure c_p

$$\chi = \frac{\lambda}{\rho c_p} \tag{3}$$

The behavior of the diffusion coefficient D near the critical mixing point and the thermal diffusivity χ near the gas-liquid critical point turns out to be rather similar. I shall occasionally refer to either quantity as diffusivity.

The phenomenon of the critical slowing down of these fluctuations is due to the fact that the diffusivity vanishes at the critical point. According to the thermodynamics of irreversible processes fluxes $\vec{J}$ of thermodynamic quantities are proportional to corresponding thermodynamic forces $\vec{X}$ [D1,H1]:

$$\vec{J} = \overleftrightarrow{L} \cdot \vec{X} , \tag{4}$$

where $\overleftrightarrow{L}$ is the matrix of Onsager phenomenological coefficients. For instance, in a binary mixture the flux $\vec{J}_i$ of component i is proportional to the gradient of its chemical potential

$$\vec{J}_i = -L\nabla\mu_i = -L\frac{\partial\mu_i}{\partial c_i}\nabla c_i \tag{5}$$

Since the diffusion coefficient is defined by Fick's law

$$\vec{J}_i = -D\nabla c_i \tag{6}$$

we see, on comparing (5) with (6), that D can be represented as the ratio of the Onsager phenomenological coefficient L, which is of a dynamical nature, over the susceptibility $\partial c/\partial\mu$ which is a static property.

$$D = L \Big/ \left(\frac{\partial c}{\partial \mu}\right)_{T,P} \tag{7}$$

In the conventional theory the critical slowing down of the fluctuations in the order parameter was wholly attributed to the divergence of the static susceptibility [V1]. That is, the transport coefficient L in (7) was assumed to remain finite at the critical mixing point, so that the diffusion coefficient would vanish as the inverse susceptibility [D2]. Similarly, the thermal conductivity λ in (3) was assumed to be finite at the gas-liquid critical point [V1], so that the thermal diffusivity would vanish as c_P^{-1} which in turn vanishes as the inverse compressibility.

That the actual dynamic processes are more complicated became apparent, when experiments revealed that the thermal conductivity λ diverges at the gas-liquid critical point [S1]. In recent years it has become evident that the temperature dependence of the diffusion coefficient of mixtures near the critical mixing point also differs essentially from the behavior predicted by the conventional theory.

In this report we shall present an analysis of experimental data for those transport properties (thermal conductivity, thermal diffusivity and binary diffusion coefficient) which determine the critical slowing down of the fluctuations of the order parameter in gases and binary liquids. This analysis will be preceded by an assessment of the experimental situation concerning the viscosity of fluids near the critical point. An earlier review of the subject has been presented elsewhere [S2]. Since this review may not be easily accessible to the reader, I have included in this report a bibliography on the subject.

In the traditional thermodynamic experiments transport properties are measured by observing the response of the system to the presence of macroscopic gradients in the thermodynamic variables. Such gradients are introduced experimentally by imposing boundary conditions on the system. To deduce the transport coefficients from the observations one needs to integrate the hydrodynamic equations for the experimental boundary conditions. Near the critical point this procedure is complicated by the fact that some of the fluid properties may vary appreciably in the system.

The spatial and temporal Fourier components of the fluctuations can be studied by observing the intensity of light scattered through the fluid as a function of scattering angle and frequency. New spectroscopic methods using laser light have thus made it possible to determine the diffusivity from the width of the Rayleigh line in the spectrum of scattered light. This second method avoids many difficulties associated with the presence of macroscopic gradients in the thermodynamic experiments, since it allows us to measure the diffusivity, while the system remains macroscopically in equilibrium. Experimental results obtained with the two procedures are in agreement as discussed in Section IV.1.

SECTION II

SHEAR VISCOSITY

1. Viscosity of Binary Liquid Mixtures

In 1901 Friedländer published a beautiful paper "Uber merkwürdige Erscheinungen in der Umgebung des kritischen Punktes" in which he demonstrated that the shear viscosity of the binary liquids phenol-water and isobutyric acid-water increases anomalously, when the critical mixing point is approached [Fl]. A few years later Scarpa reported the same phenomenon [S3]. The existence of a viscosity anomaly has been confirmed subsequently by a variety of authors. The experimental literature is summarized in Table I.

Almost all experimental data have been obtained by observing the flow rate of the liquid mixture when flowing through a capillary. The use of a capillary flow method is not without difficulties near the critical point [S2]. First, it may be difficult to attain high uniformity in the thermodynamic variables such as temperature and composition. Furthermore, the capillary flow method requires that the compressibility of the fluid is small. Recent theoretical considerations suggest that the isothermal compressibility may diverge weakly at the critical mixing point [G3,Ml]. The viscosity can also be measured by observing the damping of a cylinder oscillating or rotating in the fluid. Tsai and McIntyre have included a few data points obtained with a rotating cylinder viscometer; they appear to find the same anomalous viscosity as that obtained with the capillary flow method [Tl].

Table I

Viscosity Measurements Near the Critical Mixing Point of Binary Liquids

Authors	System
Friedländer [F1]	phenol-water isobutyric acid-water
Scarpa [S3]	phenol-water
Drapier [D3]	phenol-water isobutyric acid-water cyclohexane-aniline hexane-nitrobenzene
Semenchenko, Zorina [S4]	triethylamine-water hexane-nitrobenzene
Khazanova, Linshits [K1]	hexamethyleneimine-water
Reed, Taylor [R1]	isooctane-perfluoroheptane isooctane-perfluorocyclic oxide hexane-perfluorocyclic oxide
Zhuralev [Z1]	triethylamine-water
Debye, Chu, Woermann [D4]	cyclohexane-polystyrene
Woermann, Sarholz [W1]	isobutyric acid-water
Brunet, Gubbins [B1]	phenol-water cyclohexane-aniline cyclohexane-methanol hexane-methanol
Gvozdeva, Lyubimov [G1]	phenol-water
Arcovito et al. [A1]	cyclohexane-aniline lutidine-water
Barber, Champion [B2]	isobutyric acid-water
Allen et al. [A2,L2,S5,S6]	isobutyric acid-water 3-methylpentane-nitroethane lutidine-water
Tsai, McIntyre [T1]	3-methylpentane-nitroethane
Pings et al. [G2]	lutidine-water

An anomalous increase in the viscosity near the critical mixing point has been observed in all systems listed in Table I. It is interesting to note that the anomaly has been detected not only in systems with an upper critical solution point, but also in such systems as triethylamine-water [S4,Z1], hexamethyleneimine-water [K1] and lutidine-water [G2,S6] with a lower critical solution point.

To illustrate the behavior of the viscosity I show as an example some experimental data reported for the system 3-methylpentane-nitroethane. Fig. 1 shows the composition dependence of the viscosity according to some earlier measurements for this mixture obtained by Leister, Allegra and Allen [L1]. Near the critical point the viscosity shows a marked increase over the ideal viscosity to be expected in the absence of an anomaly.

The temperature dependence of the viscosity of many liquids can be represented by the Arrhenius equation

$$\eta = \eta_0 e^{E/RT} , \tag{8}$$

so that

$$\ell og\ \eta = A' + \frac{B'}{T} \tag{9}$$

where A' and B' are constants independent of temperature. For temperatures close to the critical temperature eqn. (9) can be approximated by

$$\ell og\ \eta = A + B\epsilon \tag{10}$$

with $\epsilon = (T-T_c)/T_c << 1$. This behavior is illustrated

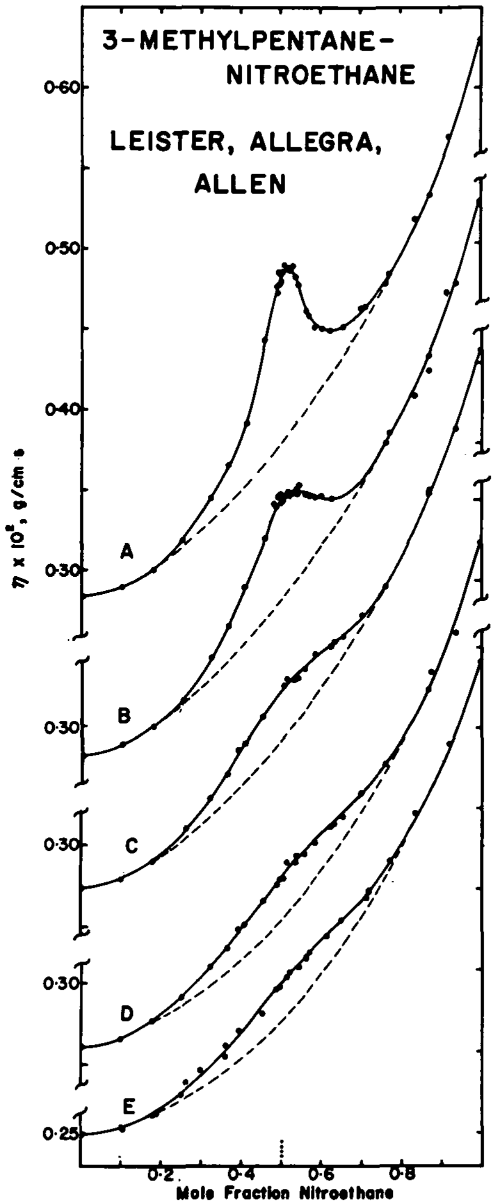

Figure 1. Viscosity of 3-methylpentane-nitroethane versus composition at several temperatures, reported by Leister, Allegra and Allen. A: $\Delta T = T - T_c = 0.044^{o}C$; B: $\Delta T = 0.544^{o}C$; C: $\Delta T = 3.555^{o}C$; D: $\Delta T = 8.544^{o}C$; E: $\Delta T = 13.465^{o}C$. The dashed line represents the estimated ideal viscosity [L1].

in Fig. 2, where the same data as shown in Fig. 1 are plotted as a function of temperature for a number of concentrations. Near the critical point the anomalous viscosity reveals itself as a deviation $\Delta\eta$ from the ideal viscosity η_{id} estimated on the basis of eqn. (10).

$$\eta = \Delta\eta + \eta_{id} \tag{11}$$

The transport coefficients are defined as the coefficients in the linear relationship between fluxes and gradients [D1,H1]. This linear relationship is only valid, when the gradients are sufficiently small. Near the critical point one should require that the variables do not change significantly over distances of the order correlation length. Since the correlation length diverges at the critical point, one may expect that the experimental viscosity will depend on the velocity gradient $\nabla\vec{v}$ sufficiently close to the critical point. In fact, Fixman and coworkers [F2, S7] suggested that the effect may be present in the thermodynamic experiments mentioned above. Woermann and Sarholz varied the shear rate $\partial v/\partial z$ near the critical point of isobutyric acid-water over about three decades and verified that the anomalous viscosity was independent of the shear rate [W1]. Tsai and McIntyre made a comprehensive study of the effect of the shear rate on the measured viscosity of 3-methylpentane-nitroethane. By complementing their capillary flow measurements with data from a rotating cylinder viscometer, they varied the shear rate over five decades from 10^{-2} sec^{-1} to 10^{+3} sec^{-1} without noting any effect on the anomalous viscosity [T1]. The fact that the anomalous viscosity does not depend on the shear rate may therefore be accepted as experimentally established for the shear rates commonly encountered in thermodynamic experiments.

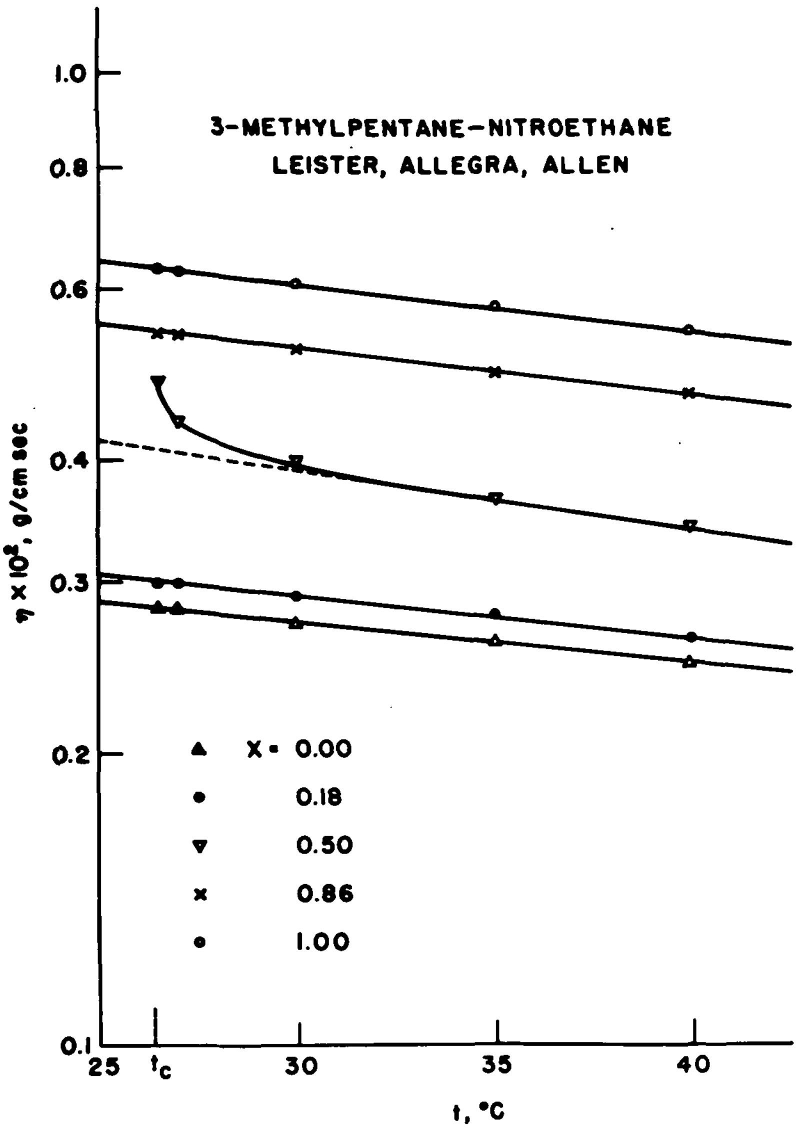

Figure 2. Log η as a function of temperature for 3-methylpentane-nitroethane at various mole fractions x of nitroethane.

The original theoretical attempts to explain the viscosity anomaly, initiated by Fixman [F2], were based on mean field considerations. The mean field theories [D5, F2,F3,M2] lead to a correlation length and viscosity both diverging as $\epsilon^{-\frac{1}{2}}$ at the critical concentration.

The experimentally observed viscosity anomaly, however, appears to be considerably weaker and may be approximated by a logarithmic divergence, as pointed out by Arcovito et al. for the viscosity of cyclohexane-aniline [A1] and lutidine-water [private communication]. The fact that the anomaly is close to logarithmic is illustrated in Fig. 3, where the anomalous viscosity $\Delta\eta$ of 3-methylpentane-nitroethane is plotted as a function of log ϵ. The figure is based on the new more precise viscosity measurements of Stein, Allegra and Allen [S5] and of Tsai and McIntyre [T1]. For an intercomparison between the two sets of data we consider a reduced anomalous viscosity $\Delta\eta^* = \Delta\eta/\eta_{id,c}$ where $\eta_{id,c}$ is the ideal viscosity at the critical point. We have thus eliminated the effect of a systematic difference of 5% between the two experiments, which is probably due to the choice of different calibration data by the two groups of investigators. It has been suggested that the anomalous viscosity approaches the behavior predicted by the mean field theories at temperatures farther away from the critical temperature [B1,L1,T1,W1]. The experimental evidence for this assertion is inconclusive [S2].

In analogy to the equilibrium properties attempts have been made to represent the anomalous viscosity by a power law

$$\eta = A\epsilon^{-\phi} + \eta_{id} \tag{12}$$

Since the anomaly is a weak one, the value deduced for the critical exponent is sensitive to the estimate for η_{id}. As the most natural choice one is inclined to identify η_{id}

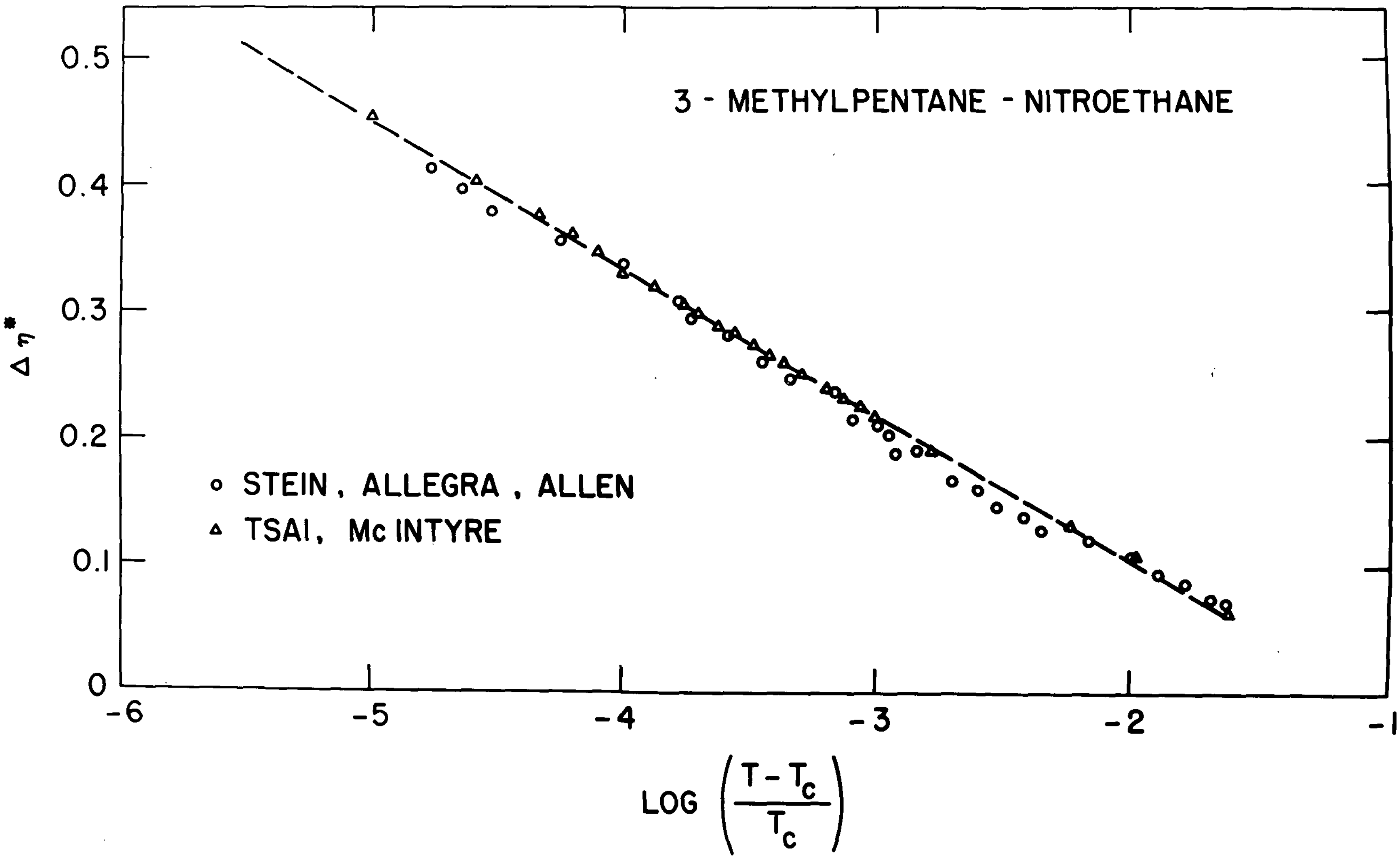

Figure 3. The anomalous viscosity $\Delta\eta^* = \Delta\eta/\eta_{id,c}$ as a function of log ϵ for a mixture of 3-methylpentane-nitroethane at the critical concentration. The data

with the viscosity values predicted by the Arrhenius equation (9) or (10), but the extrapolation can only be made with a limited precision. As an alternative η_{id} is sometimes replaced with a linear function of temperature

$$\eta = A\epsilon^{-\phi} + B\epsilon + C \ , \tag{13}$$

where, in addition to A, also B and C are treated as adjustable parameters. The coefficient A may also be a slowly varying function of temperature. Thus, the empirical function

$$\eta = e^{A+B\epsilon}\epsilon^{-\phi} \ , \tag{14}$$

introduced by Debye and coworkers [D4] may, in retrospect, be considered as an alternative procedure for determining a critical exponent.

While the viscosity anomaly was the first anomaly observed for transport properties near the critical point, it is still not well understood. Ferrell et al. [F4] and Halperin and Hohenberg [H2] have proposed an extension of the static scaling laws to include dynamical properties. More detailed predictions have been obtained by the mode-mode coupling theory developed by Kadanoff, Swift [K2,S8] and Kawasaki [K3,K4] . However, as pointed out by Kawasaki [K3], the mode-mode coupling theory implies that the viscosity will remain finite at the critical point. Since the experimental evidence for the existence of a viscosity anomaly is overwhelming, Allen et al. have attempted to reconcile the experimental observations with the theory by assuming a cusp-like behavior for the viscosity [A2,S5]

$$\eta = \frac{A}{\phi}(\epsilon^{-\phi}-1) + B\epsilon + C \ . \tag{15}$$

Recently, Kawasaki has suggested that the viscosity may follow an apparent logarithmic divergence which turns into a sharp cusp very close to the critical point [K4].

We remark that the capillary flow method yields in first instance the *kinematic* viscosity η/ρ. When the density of the liquid mixture is known, the data are usually converted into values for the *dynamic* viscosity η. It is commonly assumed that the kinematic and dynamic viscosity diverge with the same exponent. However, since the density varies with temperature, this assumption may not be true for exponents derived empirically from data in a finite temperature range. Moreover, a weakly divergent compressibility may imply an anomaly in the thermal expansion coefficient. Thus the behavior of the two viscosities may not even be the same asymptotically.

The values reported for the critical exponent of the viscosity are summarized in Table II. The fact that the anomaly is weak is reflected in the small values found for the exponent when the data are fitted to (14). However, the precise value for the exponent appears to be very sensitive to the choice for the mathematical representation. For instance, Allen et al. [L1] deduced an exponent $\phi = 0.04$ from their earlier viscosity measurements for 3-methylpentane-nitroethane when analyzed in terms of eqn. (12). On the other hand, the same data yield $\phi = -0.28 \pm 0.08$ when fitted to eqn. (15) [S5]. It is evident that the viscosity anomaly is a weak one close to logarithmic, but the mathematical character of the anomaly is not well understood.

Table II

Values Reported for the Critical Exponent of the Viscosity Near the Critical Mixing Point

System	Exponent ϕ	Equation	Reference
cyclohexane-aniline	0(log)	(a)	[A1]
	0.04	(b)	[D4, W1]
isobutyric acid-water	-0.12 ± 0.02	(c)	[A3]
	-0.37 ± 0.04	(c)	[A3, W1]
	0.05	(b)	[D4, W1]
3-methylpentane-nitroethane	-0.005 ± 0.014	(c)	[S5]
	0.03 ± 0.01		[T1]
phenol-water	0.05	(b)	[D4, W1]
hexane-nitrobenzene	0.04	(b)	[W1]
isooctane-perfluoroheptane	0.07	(b)	[D4, W1]
lutidine-water	0(log)	(a)	[Arcovito, private communication]

$$\frac{\eta}{\rho} = A\ln\epsilon + B + \left(\frac{\eta}{\rho}\right)_{id} \qquad \text{(a)}$$

$$\eta = e^{A+B\epsilon}\epsilon^{-\phi} \qquad \text{(b)}$$

$$\eta = \frac{A}{\phi}\left(\epsilon^{-\phi}-1\right) + B\epsilon + C \qquad \text{(c)}$$

2. Viscosity Near the Gas-Liquid Critical Point

The question whether the viscosity exhibits a weak anomaly near the gas-liquid critical point cannot be answered unambiguously due to a lack of reliable data sufficiently close to the critical point. The capillary flow method requires the presence of a pressure gradient which induces a large density gradient near the critical point. As a consequence the analysis of the flow pattern becomes extremely complicated and the data do not permit us to discriminate between the presence and the absence of a weak anomaly like that observed near the critical mixing point [S2].

For a study of the viscosity in the critical region the oscillating disk viscometer offers many advantages over the capillary flow viscometer. It does not require a pressure gradient and it provides a local determination of the viscosity at a particular level in the fluid. The method would be ideal, when combined with a local determination of the density, thus avoiding corrections for density gradients induced by gravity [S2].

Viscosity measurements, obtained with an oscillating disk viscometer, have been reported by Naldrett and Maass [N1] and by Kestin, Whitelaw and Zien [K5] for carbon dioxide near the critical point. Both sets of data indicate an anomalous increase in the viscosity close to the critical point. The effect is demonstrated in Fig. 4, where the experimental viscosity data at 31.2°C (corresponding to $T-T_c = 0.2^{\circ}C$) are plotted as a function of density and compared with the ideal viscosity. The ideal viscosity can be estimated from data at 40°C [K5], 50°C and 75°C [M3] by observing that the temperature dependence of the viscosity at any given density is approximately the same as

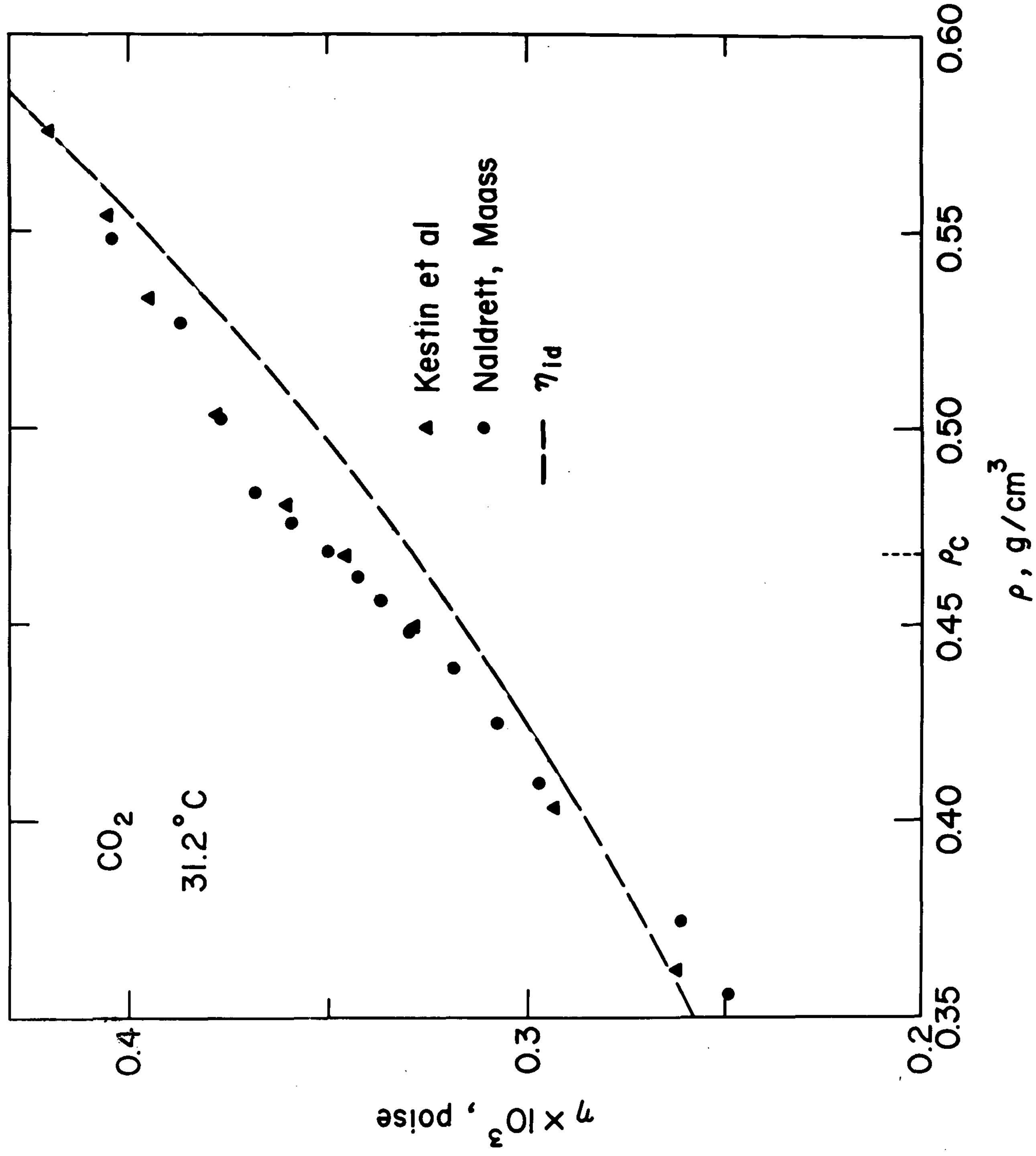

Figure 4. The viscosity of CO_2 at $T-T_c = 0.2^{o}C$ as measured by Naldrett and Maass [N1] and Kestin, Whitelaw and Zien [K5].

the temperature dependence of the viscosity in the low density limit $\rho \to 0$

$$\eta_{id}(\rho, T') - \eta_{id}(\rho, T'') = \eta(0, T') - \eta(0, T'') \qquad (16)$$

This procedure will be discussed in more detail in Section III.2, where it will also be used to estimate the ideal thermal conductivity. While the data of Naldrett and Maass and of Kestin and coworkers do provide some evidence for a weak anomaly in the viscosity, they do not permit any conclusion concerning the mathematical character of the anomaly.

Diller [D6] and Herreman et al. [H3] have studied the viscosity of, respectively, hydrogen and carbon dioxide in the supercritical region by observing the damping of a torsionally vibrating piezoelectric crystal. However, the resolution of these experiments is insufficient to determine the presence or absence of a weak anomaly as observed by Kestin et al. Additional experimental information is needed to decide whether the viscosity near the gas-liquid critical point exhibits an anomaly similar to that observed near the critical mixing point.

SECTION III

THERMAL CONDUCTIVITY NEAR THE GAS-LIQUID CRITICAL POINT

1. Survey of Experiments

The thermal conductivity of compressed gases is usually measured either with a concentric cylinder method or with a parallel plate method. In both methods a temperature difference is established across a layer of the fluid and the heat flow is measured in the stationary state as a function of the temperature gradient ∇T. In the first method the fluid is enclosed between two concentric cylinders either in horizontal or in vertical position and heat is generated in the inner cylinder; in the second method the fluid is enclosed between two parallel horizontal plates and the heat is flowing from the upper plate to the lower plate [S2].

Near the critical point special precaution is needed to avoid errors due to the presence of natural convection. When the convection is small, the error in the apparent thermal conductivity coefficient is estimated to be proportional to the Rayleigh number [M4]

$$N_{Ra} = \frac{g\alpha_p \rho^2 c_p d^3 \nabla T}{\lambda\eta} \tag{17}$$

Here g is the gravitation constant, $\alpha_p = -\rho^{-1}(\partial\rho/\partial T)_p$ the thermal expansion coefficient and d the thickness of the gas layer. The Rayleigh number is strongly divergent at the critical point, since both α_p and c_p diverge as the isothermal compressibility. The convection also increases with the angle between the direction of gravity $\vec{g}$ and the density gradient which accompanies the temperature gradient. The parallel plate configuration is therefore the more favorable configuration for avoiding convection.

Evidence for the existence of a thermal conductivity anomaly near the critical point of carbon dioxide was presented by Guildner on the basis of data obtained with a concentric cylinder method [G4]. A comprehensive study of the thermal conductivity of carbon dioxide was made by the author in collaboration with Michels and Van der Gulik [M4,M5]. The experimental results, obtained with a parallel plate apparatus, are shown in Fig. 5. It could be established that the experimental thermal conductivity coefficient was independent of the value of the Rayleigh number. We, therefore, concluded that the anomaly could not be attributed to convection and that the anomalous heat conduction satisfied the law of Fourier.

The existence of a thermal conductivity anomaly was subsequently confirmed by Needham and Ziebland for ammonia [N2]. The densities to be associated with their experimental data were recently recalculated by Haar and coworkers using a more up to date representation of the P-V-T surface of NH_3.† The results are shown in Fig. 6. In retrospect, some evidence for an anomalous behavior of the thermal conductivity could also be detected in earlier measurements for argon and nitrogen [S9].

A survey of the experimental literature is presented in Table III. It appears that the existence of a thermal conductivity anomaly has been verified for helium [K6], argon [B3,S9], xenon [T2], hydrogen [R2], carbon dioxide [G4,L4,M4,M5], ammonia [N2], sulfurhexafluoride [L3] and

† L. Haar, National Bureau of Standards, private communication.

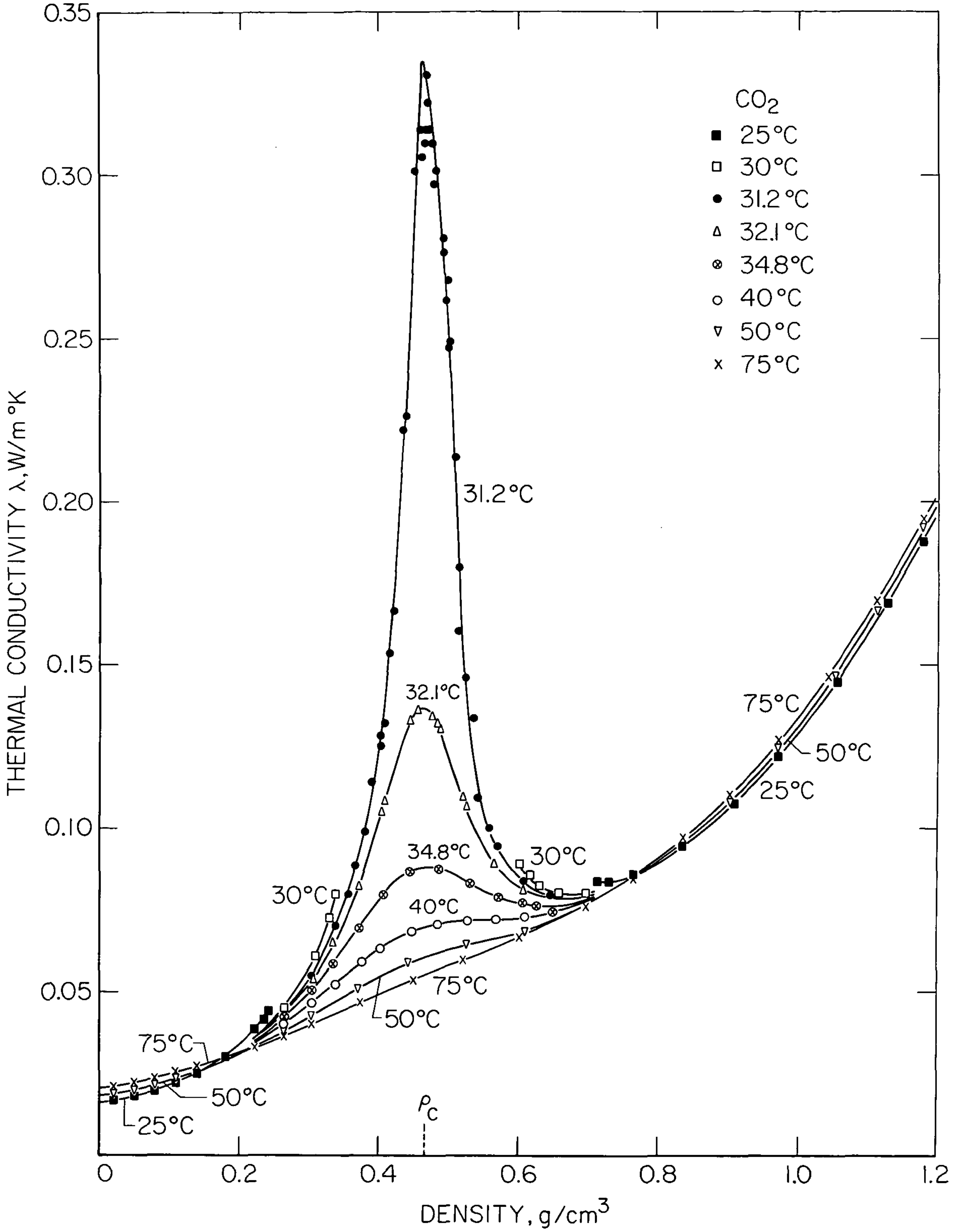

Figure 5. The thermal conductivity of CO_2 as a function of density and temperature ($T_c \simeq 31.00^oC$).

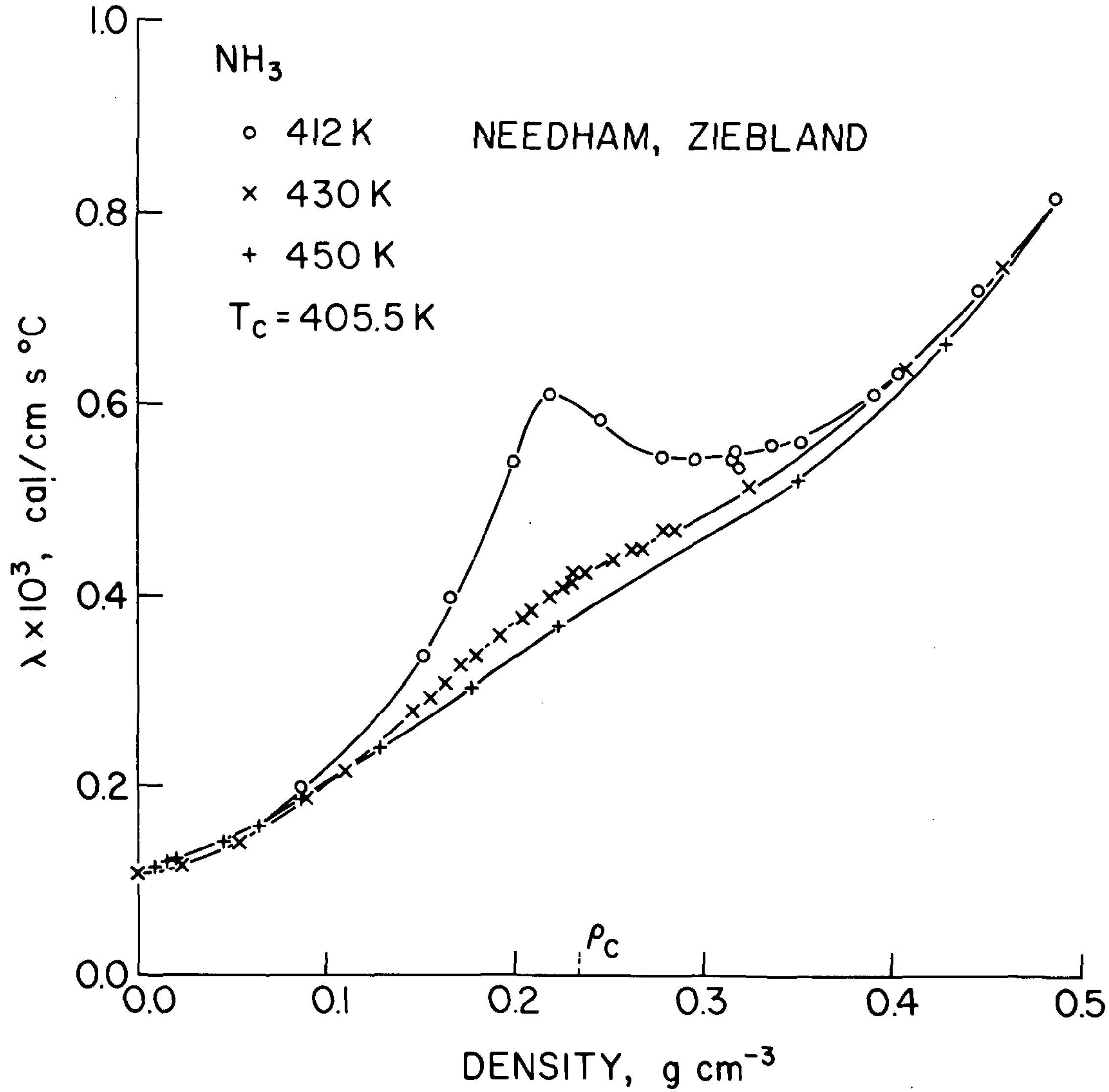

Figure 6. The thermal conductivity of ammonia in the supercritical region as a function of density. The curves are deduced from the experimental data obtained by Needham and Ziebland [N2].

Table III

Thermal Conductivity Measurements in the Critical Region of Gases

Investigators	Method	Substance
Guildner [G4]	vertical cylinder	carbon dioxide
Michels, Sengers [M4,M5,S10]	parallel plate	carbon dioxide
Amirkhanov, Adamov [A4,V2]	parallel plate vertical cylinder	carbon dioxide
Simon, Eckert [S11]	interferometer	carbon dioxide
Ziebland, Burton [Z2,S9]	vertical cylinder	nitrogen
Ikenberry, Rice [I1,S9]	vertical cylinder	argon
Needham, Ziebland [N2]	vertical cylinder	ammonia
Golubev, Sokolova [G5,S12]	vertical cylinder	ammonia methane
Lis, Kellard [L3]	vertical cylinder	sulfurhexafluoride
Bailey, Kellner [B3]	vertical cylinder horizontal cylinder	argon
Kerrisk, Keller [K6]	parallel plate	helium
Roder, Diller [R2]	parallel plate	hydrogen
Murthy, Simon [M6]	parallel plate	carbon dioxide
Le Neindre et al. [L4, T2]	concentric cylinder	carbon dioxide steam xenon

steam [Le Neindre et al.]. I believe that Amirkhanov and Adamov did not approach the critical point sufficiently closely and that the measurements of Golubev and Sokolova may have been affected by convection. Using a corresponding state argument it can be shown that the anomalies observed in argon, nitrogen, carbon dioxide and ammonia are all of the same order of magnitude [S2]. The measurements of Murthy and Simon for CO_2 do not agree with our data.

2. Interpretation in Terms of Scaling Laws

In this and the subsequent section I shall present an analysis of our thermal conductivity data for carbon dioxide. For this purpose I have selected values for a number of parameters such as critical temperature and critical exponents which may not be definitive. This analysis is a preliminary one and details may be subject to minor revisions.

We first recall that the equilibrium thermodynamic properties satisfy static scaling laws. These scaling laws follow from the hypothesis, first proposed by Widom [W2] and elucidated by Griffiths [G6], that the Helmholtz free energy is a homogeneous function of its characteristic variables. In this formulation the chemical potential can be represented in the form

$$\frac{\mathrm{sign}(\Delta\rho^*)\,\Delta\mu^*}{|\Delta\rho^*|^{\delta}} = h(x) \tag{18}$$

where h(x) is a function of a variable x defined by

$$x = \frac{\epsilon}{|\Delta\rho^*|^{1/\beta}} \tag{19}$$

In these equations $\Delta\mu^*$ is a reduced chemical potential difference $\Delta\mu^* = \{\mu(\rho,T) - \mu(\rho_c,T)\}\rho_c/P_c$, $\Delta\rho^*$ a reduced density $\Delta\rho^* = (\rho-\rho_c)/\rho_c$, δ the exponent of the critical isotherm and β the exponent of the coexistence curve. The function h(x) should satisfy a number of conditions formulated by Griffiths [G6]. I refer to the left hand side of (18) as the "scaled" chemical potential. The principle of thermodynamic scaling thus implies that the scaled chemical potential is a function of a single scaling parameter x. The validity of this scaling law relation has been experimentally verified for a variety of gases and magnets [M7,M8,S13].

Fig. 7, taken from reference [M7], shows the scaled chemical potential, deduced from the experimental P-V-T data of Michels and coworkers for CO_2 [M9], as a function of $(x+x_0)/x_0$. The solid curve represents an equation for h(x) proposed by Vicentini-Missoni, Levelt Sengers and Green [M7]

$$h(x) = E_1\left(\frac{x+x_0}{x_0}\right)\left[1+E_2\left(\frac{x+x_0}{x_0}\right)^{2\beta}\right]^{\frac{\gamma-1}{2\beta}} \tag{20}$$

with the following parameters for CO_2

$$\begin{array}{llll} \beta = 0.35 & & P_c/\rho_c = 0.3075 \text{ atm/Amagat} & \\ \gamma = 1.26 & & x_0 = 0.135 & \\ T_c = 304.11 \text{ K} & & E_1 = 2.35977 & \\ \rho_c = 236.7 \text{ Amagat}^{\dagger} & & E_2 = 0.29684 & \text{(20a)} \end{array}$$

---

†In this report the density is occasionally expressed in terms of Amagat units. The density in Amagat is the actual density relative to the density of the same substance at 0^oC and 1 atmosphere. For CO_2 1 Amagat = 0.0019764 g/cm^3.

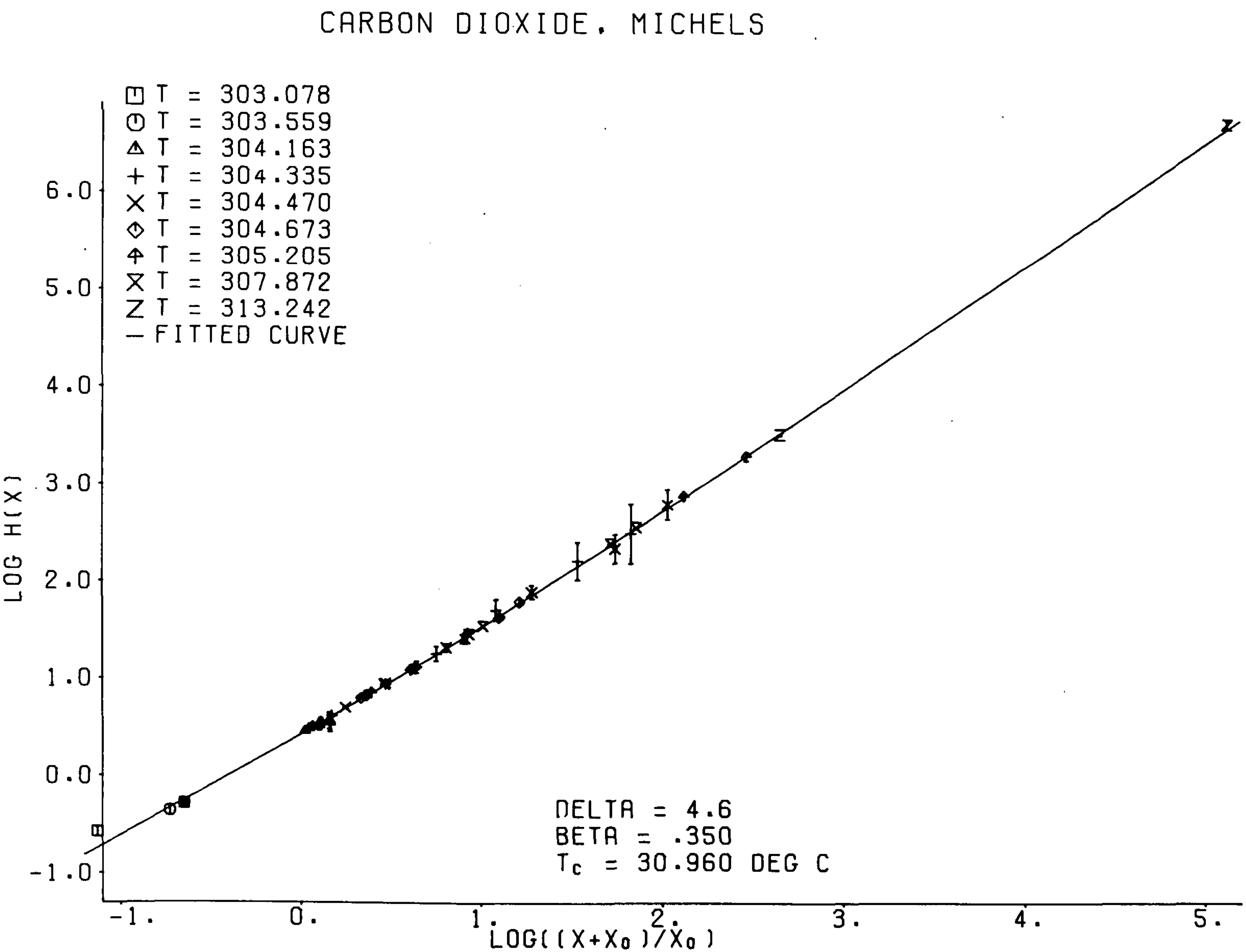

Figure 7. Log-log plot of the scaled chemical potential $h(x)$ versus $(x+x_0)/x_0$ for CO_2 [M7].

The parameter x_0 is defined such that the line $x = -x_0$ represents the coexistence curve. In preparing this report I found some evidence that the authors may have slightly underestimated the value of the critical temperature to be attributed to the data of Michels and coworkers by a few hundredths of a degree. Nevertheless, for the present purpose I have continued to use the NBS equation (20) with parameters (20a), since they provide a good representation of the chemical potential at the temperatures and densities at which the thermal conductivity was measured. The simple scaling law relation is valid in a range covering approximately ±30% in reduced densities and at reduced temperatures up to 3% above the critical temperature.

The scaling law relation (18) for the chemical potential implies similar scaling law relations for the other thermodynamic properties. In general, an anomalous thermodynamic property $X(\rho,T)$ that diverges along the critical isochore with an exponent ψ

$$X(\rho_c, T) = X_0 |\epsilon|^{-\psi} \tag{21}$$

can be written in the form

$$\frac{A_X^*(\rho) X(\rho,T)}{X_0 |\Delta\rho^*|^{-\psi/\beta}} = f_X(x) \tag{22}$$

where $f_X(x)$ is again a function of the scaling parameter x. The factor $A_X^*(\rho)$ accounts for any asymmetry of X around the critical density ρ_c. In principle, this asymmetry factor A_X^* will be a function of both ρ and T. However, since the validity of the power law (21) and the scaling law (22) is limited to a range of about 3% in the temperature variable, the temperature dependence of the coefficient X_0 in (21), and consequently that of the factor A_X^* is usually neglected, as we shall do also in the present report.

As an example of (22) let us consider the isothermal compressibility K_T which diverges with the exponent γ

$$K_T^*(\rho_c, T) = \Gamma|\epsilon|^{-\gamma} \tag{23}$$

The coefficient Γ is related to the parameters in the NBS equation (20)

$$\Gamma^{-1} = x_0^{-\gamma} E_1 E_2^{(\gamma-1)/2\beta} \tag{24}$$

when K_T is expressed in dimensionless units $K_T^* = P_c K_T$. Since $\rho^2 K_T = (\partial\rho/\partial\mu)_T$, it follows from (18) that the compressibility will scale after multiplication with ρ^2:

$$\frac{\rho^{*2} K_T}{\Gamma|\Delta\rho^*|^{-\gamma/\beta}} = f_{K_T}(x) = \Gamma^{-1}\{\delta h(x) - \frac{x}{\beta}h'(x)\}^{-1} \tag{25}$$

The validity of (25) is demonstrated for CO_2 in Fig. 8, where scaled values of the compressibility are plotted as a function of $(x+x_0)/x_0$. The data points represent compressibility values which were earlier deduced from P-V-T data by numerical differentiation; the solid curve was obtained by substituting the NBS equation (20) with parameters (20a) into the right hand side of (25). The agreement between the two procedures for calculating the compressibility gives additional support to the adequacy of the chosen representation for the thermodynamic properties at the temperatures under consideration.

The origin of the scaling laws is associated with the fact that the anomalous thermodynamic properties are functions of a single correlation length ξ [K7]. In the

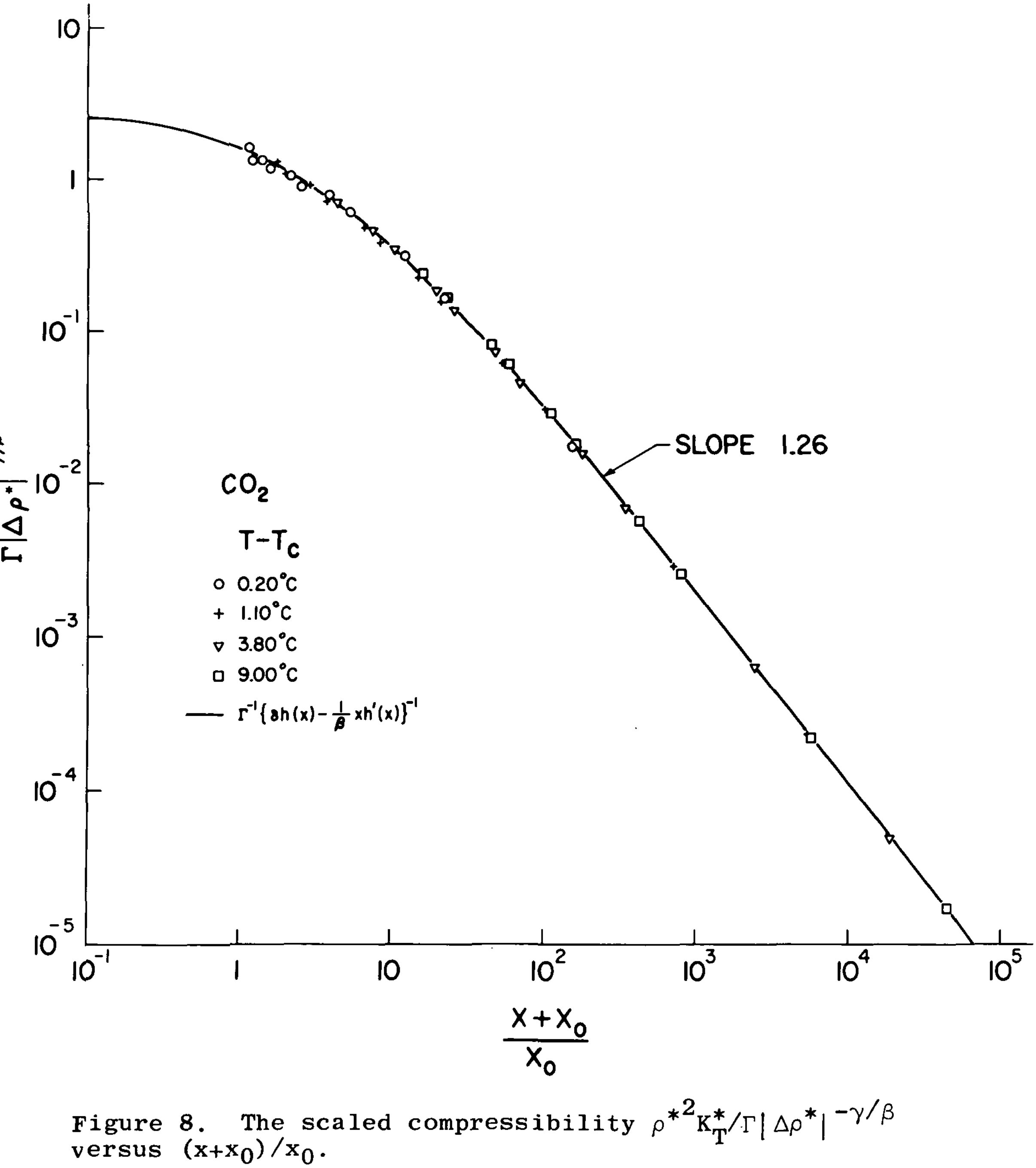

Figure 8. The scaled compressibility $\rho^{*2}K_T^*/\Gamma|\Delta\rho^*|^{-\gamma/\beta}$ versus $(x+x_0)/x_0$.

hydrodynamic limit we may expect that the anomalous thermal conductivity will be determined by the same correlation length. This consideration led us to investigate in an earlier study with Keyes, whether the thermal conductivity would satisfy a scaling law relation similar to that established for the equilibrium thermodynamic properties [S14].

In analogy to the viscosity of binary liquid mixtures we separate the experimental thermal conductivity λ into an anomalous part $\Delta\lambda$ and an ideal part λ_{id}

$$\lambda = \Delta\lambda + \lambda_{id} \tag{26}$$

The ideal or background thermal conductivity λ_{id} is estimated empirically by extrapolating data away from the critical point into the critical region. For this purpose it is convenient to consider a so-called excess thermal conductivity

$$\tilde{\lambda} = \lambda(\rho,T) - \lambda(0,T) \tag{27}$$

which measures the excess of the actual thermal conductivity $\lambda(\rho,T)$ at density ρ over the value $\lambda(0,T)$ in the low density limit $\rho \to 0$ at the same temperature. Many previous investigators have noted that this excess thermal conductivity $\tilde{\lambda}$ is to a good approximation independent of the temperature at densities up to twice the critical density [S15]. This phenomenon is illustrated for carbon dioxide in Fig. 9, based on the experimental data of Le Neindre and coworkers [L4]. The data in this figure correspond to a range of temperatures from 200°C to 700°C; no systematic trend with temperature can be detected. Once $\tilde{\lambda}$ is established as a function of ρ from data outside the critical region, the

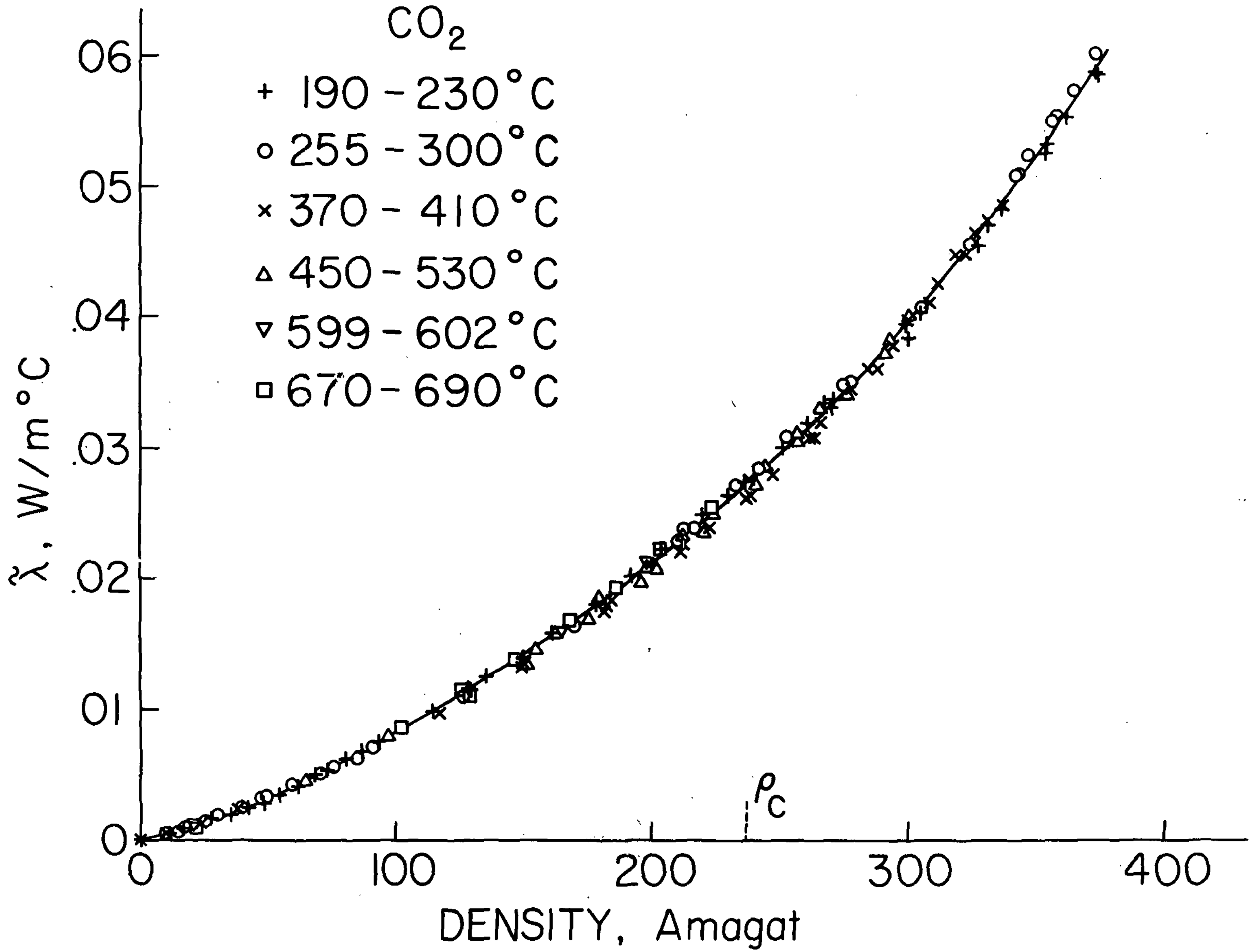

Figure 9. The excess thermal conductivity $\tilde{\lambda} = \lambda(\rho,T) - \lambda(0,T)$ for CO_2 as a function of density, deduced from the experimental data of Le Neindre et al [L4].

ideal thermal conductivity in the critical region can be calculated as

$$\lambda_{id} = \tilde{\lambda}(\rho) + \lambda(0,T) \tag{28}$$

In the absence of reliable information the thermal conductivity near the critical point has often been identified with the ideal thermal conductivity (28) in the engineering literature [K8].

The experimental data of Le Neindre et al. are in good agreement with our thermal conductivity data in the region of overlap [L4,S2]. Thus we can use these high temperature data with some confidence for estimating the background term in our thermal conductivity data. Approximating $\tilde{\lambda}(\rho)$ by a cubic polynomial, the ideal thermal conductivity for CO_2 is estimated as

$$\lambda_{id}(\rho,T) = \lambda(0,T) + \lambda_1\rho + \lambda_2\rho^2 + \lambda_3\rho^3 \tag{29}$$

with

$$\lambda_1 = 0.6678 \times 10^{-4}\ \mathrm{W/m^oC\ am}$$
$$\lambda_2 = 1.083 \times 10^{-7}\ \mathrm{W/m^oC\ am^2}$$
$$\lambda_3 = 3.659 \times 10^{-10}\ \mathrm{W/m^oC\ am^3}$$

The anomalous thermal conductivity $\Delta\lambda = \lambda - \lambda_{id}$, thus deduced from our experimental data, is shown in Fig. 10. Values for $\Delta\lambda$ are listed in Table IV for those densities and temperatures at which the validity of the scaling laws have been previously verified for the equilibrium properties. These values were obtained from data presented in Table XIV of the original publication [M5].

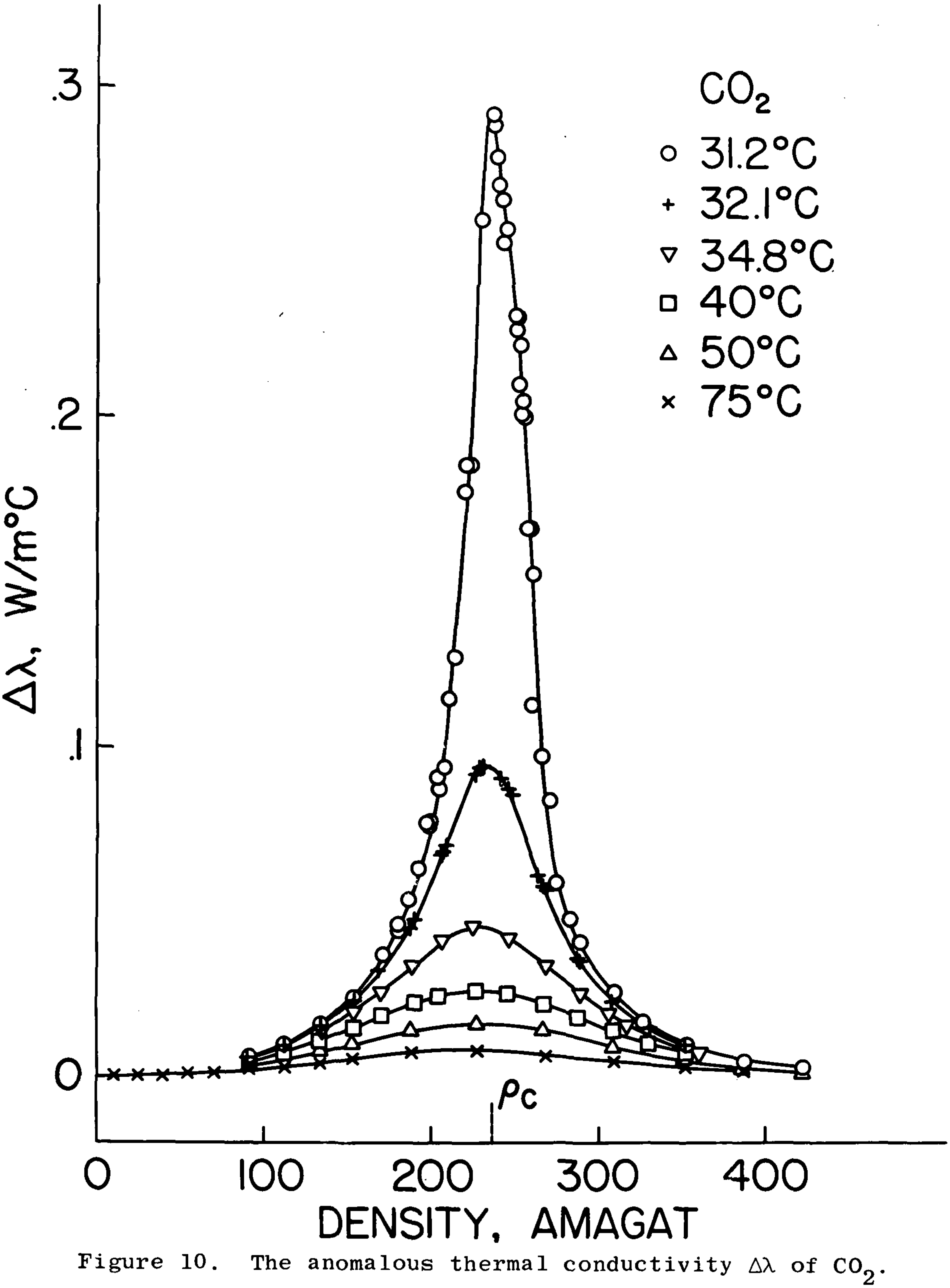

Figure 10. The anomalous thermal conductivity $\Delta\lambda$ of CO_2.

Table IV

Anomalous Thermal Conductivity of Carbon Dioxide in the Critical Region*

	$\Delta\lambda$, W/m°C			
ρ amagat \ $T-T_c$	0.20°C	1.10°C	3.80°C	9.00°C
170	0.0364	0.0318	0.0257	0.0185
190	0.0590	0.0490	0.0348	0.0225
200	0.0798	0.0609	0.0392	0.0243
210	0.115	0.0744	0.0428	0.0256
220	0.189	0.0882	0.0449	0.0261
230	0.267	0.0957	0.0453	0.0262
240	0.282	0.0931	0.0439	0.0256
250	0.230	0.0820	0.0412	0.0245
260	0.132	0.0667	0.0372	0.0231
270	0.0752	0.0525	0.0327	0.0213
290	0.0395	0.0332	0.0245	0.0173
310	0.0240	0.0218	0.0180	0.0135

*ρ_c = 237 amagat.

To investigate whether $\Delta\lambda$ satisfies a scaling law relation of the form (22) we first represent the temperature dependence of $\Delta\lambda$ along the critical isochore by a power law (21)

$$\Delta\lambda(\rho_c, T) = \Lambda\epsilon^{-\psi} \tag{30}$$

The values of $\Delta\lambda$ at the critical isochore, estimated by interpolating the experimental data, are plotted as a function of ϵ on a logarithmic scale in Fig. 11. They do satisfy the power law (30) with parameters

$$\Lambda = (0.0028 \pm 0.0003)\ \mathrm{W/m^{o}C}, \quad \psi = 0.63 \pm 0.03 \tag{31}$$

corresponding to $t_c = (31.00 \pm 0.04)^{o}C$. The precision of the values determined for these parameters is limited by some uncertainty in the value of the critical temperature to be used in the interpretation of the measurements. In this report the thermal conductivity data are analyzed in terms of $t_c = 31.00^{o}C$; however, they can also be described satisfactorily in terms of $t_c = 31.04^{o}C$ as shown earlier [S2,S14]. The errors quoted in (31) correspond to an estimated uncertainty of $\pm 0.04^{o}C$ in the value of t_c.

In analogy to (22) we now conjecture

$$\frac{A_\lambda^*(\rho)\Delta\lambda}{\Lambda|\Delta\rho^*|^{-\psi/\beta}} = f_\lambda(x) \tag{32}$$

The presence of an asymmetry factor A_λ^* manifests itself in a shift of the peaks in Fig. 10 to lower densities, when the temperature is increased. This asymmetry factor may be a complicated, but nonsingular, function of density

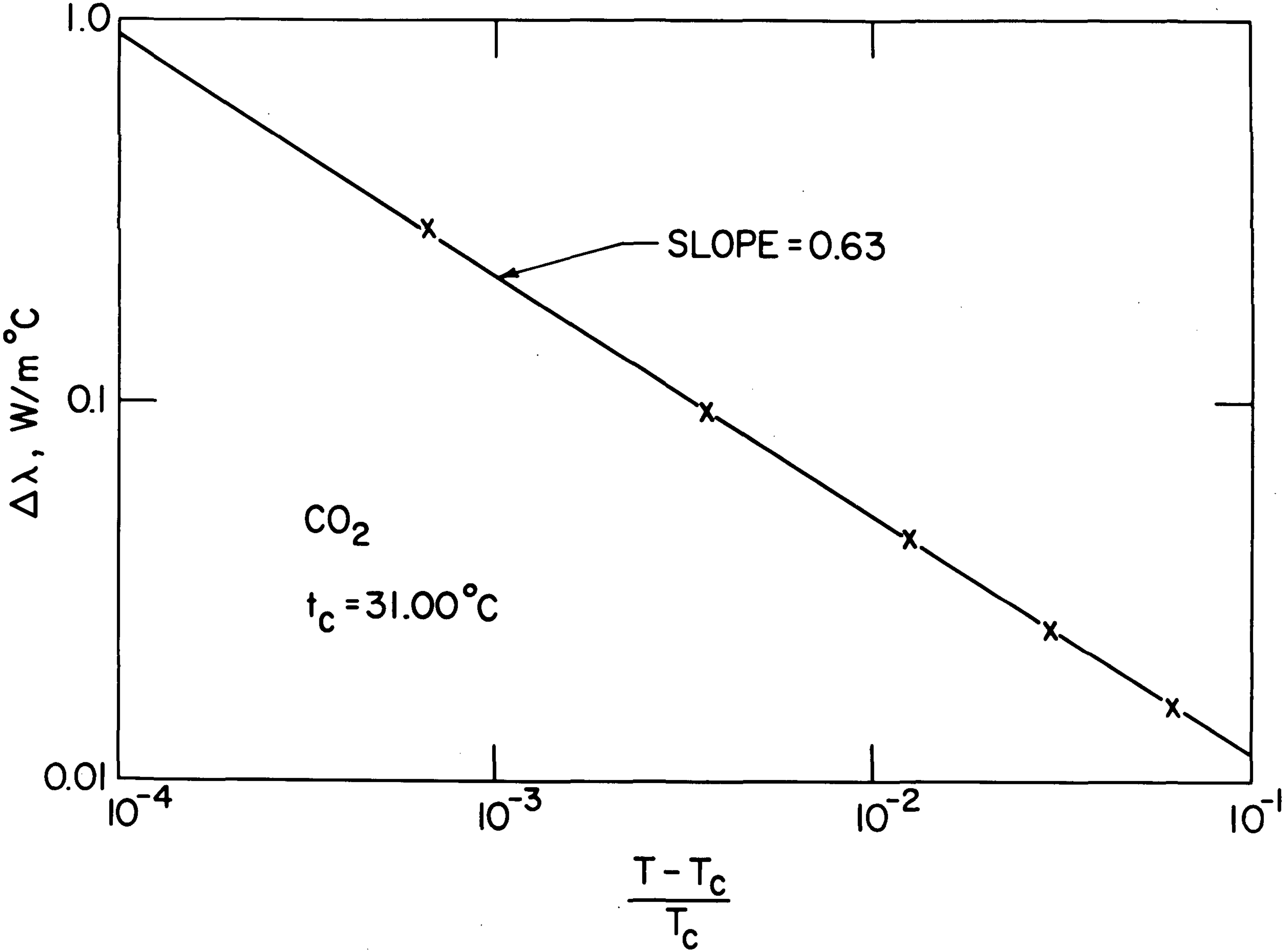

Figure 11. Log-log plot of $\Delta\lambda$ of CO_2 as a function of $\epsilon = (T-T_c)/T_c$ at the critical isochore $\rho = \rho_c$.

(and temperature). However, we have noticed empirically that it can be approximated by $A_\lambda^*(\rho) = \sqrt{\rho^*}$ [S14].

$$\frac{\rho^{*\frac{1}{2}}\Delta\lambda}{\Lambda|\Delta\rho^*|^{-\psi/\beta}} \cong f_\lambda(x) \tag{33}$$

In Fig. 12 we have plotted the empirical values of $\rho^{*\frac{1}{2}}\Delta\lambda/\Lambda|\Delta\rho^*|^{-\psi/\beta}$ as a function of $(x+x_0)/x_0$ for the parameters $\Lambda = 0.00278$ W/m^{o}C, $\psi = 0.63$, $\beta = 0.35$, $t_c = 31.00^oC$ and $\rho_c = 236.7$ amagat. The data points correspond to the values listed in Table IV; they cover the same range in densities and temperatures for which the scaled compressibility was shown in Fig. 8. Fig. 12 confirms that the scaled thermal conductivity to a good approximation can indeed be represented by a single valued function of the scaling parameter x.

In an attempt to investigate the nature of the scaling function $f_\lambda(x)$ for the thermal conductivity, I shall assume that the correlation length ξ can be approximated by the Ornstein-Zernike formula [F5,M10]

$$\xi = R\sqrt{nk_BTK_T} \tag{34}$$

where n is the number density, k_B Boltzmann's constant and R a proportionality constant, usually referred to as short range correlation length. I shall also assume that this short range correlation length is constant throughout the critical region. The Ornstein-Zernike formula (34) implies $\nu = \gamma/2$, where ν is the critical exponent for the correlation length ξ

$$\xi = \xi_0\epsilon^{-\nu} \tag{35}$$

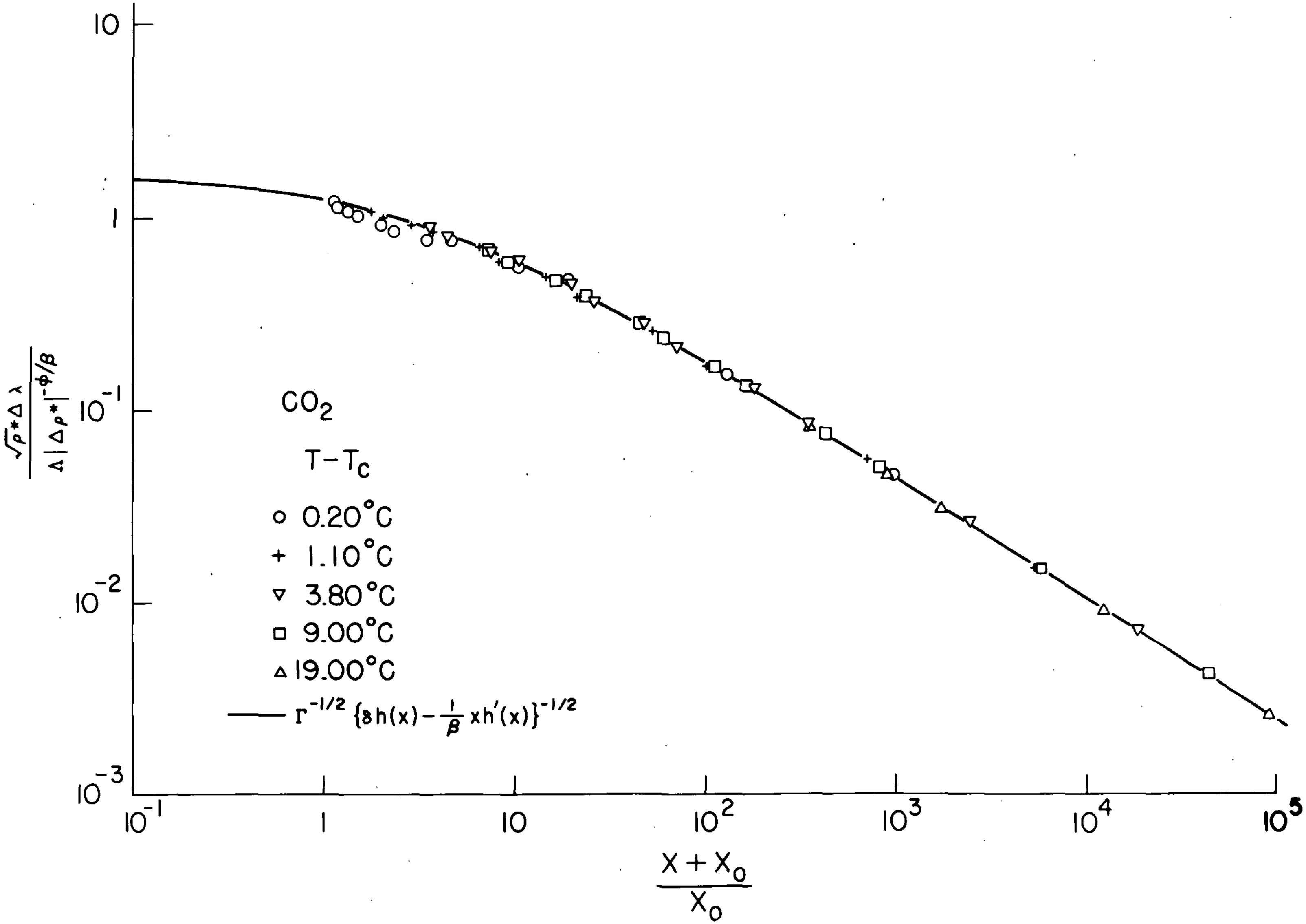

Figure 12. The scaled thermal conductivity $\sqrt{\rho^*}\Delta\lambda/\Lambda|\Delta\rho^*|^{-\psi/\beta}$ as a function of $(x+x_0)/x_0$ for CO_2. The solid curve represents the scaled correlation length $\sqrt{\rho^*}\xi/\xi_0|\Delta\rho^*|^{-\nu/\beta}$.

On comparing (35) with (23) and (34) we note that the coefficient ξ_0 can be identified as

$$\xi_0 = R\sqrt{nk_B T\Gamma/P_c} \cong R\sqrt{nk_B T_c \Gamma/P_c} \qquad (36)$$

where Γ is again given by (24). The Ornstein-Zernike theory is not exact, but deviations are known to be minor. Furthermore, since K_T in (34) will be evaluated from the NBS equation with $\gamma = 1.26$, we obtain $\nu = 0.63$ in good agreement with the value $\nu = 0.63 \pm 0.01$ recently determined experimentally by Lunacek and Cannell for CO_2 [L5].

If we substitute (25) into (34) and neglect the secular temperature dependence in the expression (36) for ξ_0, we see that the correlation length ξ scales after multiplication with $\sqrt{\rho^*}$:

$$\frac{\rho^{*\frac{1}{2}}\xi}{\xi_0|\Delta\rho^*|^{-\nu/\beta}} = f_\xi(x) = \Gamma^{-\frac{1}{2}}\{\delta h(x) - \frac{x}{\beta}\, h'(x)\}^{-\frac{1}{2}} \qquad (37)$$

The scaled correlation length can be calculated by substituting the NBS equation (20) for h(x) into (37). The results thus obtained are represented by the solid curve in Fig. 12. I emphasize, therefore, that the curve in Fig. 12 was not fitted to the experimental thermal conductivity data, but obtained from an independent calculation of the equilibrium correlation length. It turns out that within the resolution of the experimental data the scaling function for ξ coincides with the scaling function found empirically for $\Delta\lambda$. Thus we conclude that in the range of simple scaling to a good approximation

$$\frac{\rho^{*\frac{1}{2}}\Delta\lambda}{\Lambda|\Delta\rho^*|^{-\psi/\beta}} \cong \frac{\rho^{*\frac{1}{2}}\xi}{\xi_0|\Delta\rho^*|^{-\nu/\beta}} \qquad (38)$$

which, combined with $\psi = \nu = 0.63$, implies that

$$\Delta\lambda \propto \xi \tag{39}$$

3. Comparison With the Mode-Mode Coupling Theory

In the early attempts to explain the thermal conductivity anomaly the enhancement was attributed to the association and dissociation of clusters diffusing in the presence of a temperature gradient [P1] in obvious analogy to the increased thermal conductivity observed in dissociating gases [B4]. This approach was pursued to an admirable degree by Brokaw in a report that may not have received sufficient attention [B5]. To obtain quantitative agreement with experiment, however, one needs to introduce various empirical adjustments [H4].

An alternate but less realistic prediction $\lambda \propto \epsilon^{-\frac{1}{2}}$ was provided by the mean field theories [F3,M2]. Since in these mean field theories the correlation length ξ and the heat capacity c_v also diverge as $\epsilon^{-\frac{1}{2}}$, this result can also be interpreted either as $\lambda \propto \xi$ or $\lambda \propto c_v$. An empirical attempt to relate the thermal conductivity anomaly to the anomalous behavior of c_v and η via the Eucken factor $\lambda/\eta c_v$ [M5,S9] had to be abandoned, since it was based on erroneous viscosity measurements.

The two approaches mentioned above have now converged. Using a non-linear perturbation technique [Z3], often referred to as mode-mode coupling theory, Kadanoff and Swift [K2,S7] predicted $\lambda \propto \epsilon^{\nu-\gamma}$. The theory was further developed by Kawasaki [K3] who derived for the thermal diffusivity near the gas-liquid critical point

$$\frac{\lambda}{\rho c_p} = \frac{k_B T}{6\pi\bar{\eta}\xi} \tag{40}$$

and a similar expression for the binary diffusion near the critical mixing point

$$D = \frac{k_B T}{6\pi\bar{\eta}\xi} \tag{41}$$

The parameter $\bar{\eta}$ represents the shear viscosity which is assumed to be independent of ξ and the wave number k. These formulas have a simple physical meaning, if one imagines that the diffusion is determined by the mobility of clusters of spatial extent ξ [A1,K9]. According to the Einstein relation $D = k_B T/\zeta$, where ζ is a friction coefficient. If one identifies this friction coefficient with the hydrodynamic friction coefficient $\zeta = 6\pi\eta\xi$ as predicted by Stokes' law for a spherical droplet with radius ξ [L6], one recovers eqn. (41) for the diffusion coefficient. Near the gas-liquid critical point this formula does not apply to the mass diffusion coefficient, but to the thermal diffusivity, since the dynamical slowing down of the fluctuations is determined by the diffusion of entropy.

In order to compare (40) with experiment, we note that the theory refers to the anomalous contribution $\Delta\lambda$ to the thermal conductivity. We also remark that

$$c_p = T\rho^{-1}\left(\frac{\partial P}{\partial T}\right)_\rho^2 K_T + c_v \tag{42}$$

does not diverge with a simple power law, but contains a strongly divergent term proportional to K_T and a weakly divergent c_v. We replace c_p by c_p-c_v whose asymptotic behavior is the same as that of c_p. Thus we interpret (40) to imply

$$\Delta\lambda = \frac{k_B T}{6\pi\eta\xi}\,\rho(c_p-c_v) \tag{43}$$

The subtraction of the background c_v from c_p is not a serious limitation, since c_p diverges much faster than c_v. However, we note empirically that this procedure enlarges somewhat the range of temperatures where (43) is applicable.

The theoretical assumption that the viscosity is independent of k and ξ is probably not justified sufficiently close to the gas-liquid critical point and certainly not close to the critical mixing point. As a result there exists some ambiguity at those temperatures where η is anomalous, whether the parameter $\bar{\eta}$ should be identified with the ideal viscosity η_{id}, with the hydrodynamic viscosity or with an intermediate value. The issue is complicated by the fact that the viscosity appears in the theory under an integral over Fourier space whose major contributions arise from wave numbers $k \approx \xi^{-1}$ [K3]. In (43) we have identified $\bar{\eta}$ with the experimental viscosity η. This procedure is justified, since the anomalous contribution to the viscosity is negligibly small at the temperatures where λ was measured. The difference between ideal and full viscosity, as measured by Kestin et al.[K5] amounts to at most 5% at the temperature $\Delta T = 0.2^{\circ}$ closest to the critical temperature.

Eqn. (43) implies that $\Delta\lambda$ at the critical isochore will diverge with exponent $\psi = \gamma - \nu$. The temperature dependence (31) of the experimental $\Delta\lambda$ is consistent with this prediction. Using (34) and (42) we can also deduce from (43) a relationship between $\Delta\lambda$ and the scaling function (25) for the compressibility.

$$\frac{A_{\lambda}^{*}(\rho)\Delta\lambda}{\Lambda|\Delta\rho^{*}|^{-\psi/\beta}} = \left[\frac{\rho^{*2}K_T^{*}}{\Gamma|\Delta\rho^{*}|^{-\gamma/\beta}}\right]^{\frac{1}{2}} \tag{44}$$

where

where

$$A_\lambda^*(\rho) = \frac{A_\lambda(\rho)}{A_\lambda(\rho_c)} \tag{45a}$$

with

$$A_\lambda(\rho) = \rho^{3/2}\eta/\left(\frac{\partial P}{\partial T}\right)_\rho^2 \tag{45b}$$

In the derivation of (45) I have approximated the factor $T^{3/2}$ by a constant.

On comparing with (25) we see that relation (44) is identical to (37) and (38) except that the simple asymmetry factor $\sqrt{\rho^*}$ is to be replaced with the more complicated expression (45) for A_λ^*. This quantity can be calculated using values for $(\partial P/\partial T)_\rho$ deduced from the compressibility isotherms [M9] and the experimental viscosities measured by Kestin et al. [K5]; the results thus obtained are plotted in Fig. 13. It turns out that A_λ^* is a function of both density and temperature. However, if we want to neglect the temperature variation of this coefficient, as we have done at several stages, we see that on the average A_λ^* can be approximated by $\sqrt{\rho^*}$. Thus the relationship between $\Delta\lambda$ and the equation of state derived empirically in the previous section, can be obtained from the mode-mode coupling theory, if

(a) we neglect any deviations from the Ornstein-Zernike theory and if

(b) we approximate the asymmetry factor (45) by $\sqrt{\rho^*}$

As a last step we may ask whether (43) describes the experimental $\Delta\lambda$ also on an absolute basis. For this purpose we need an estimate for the short range correlation length R in (34). Chu and Lin have published some experimental

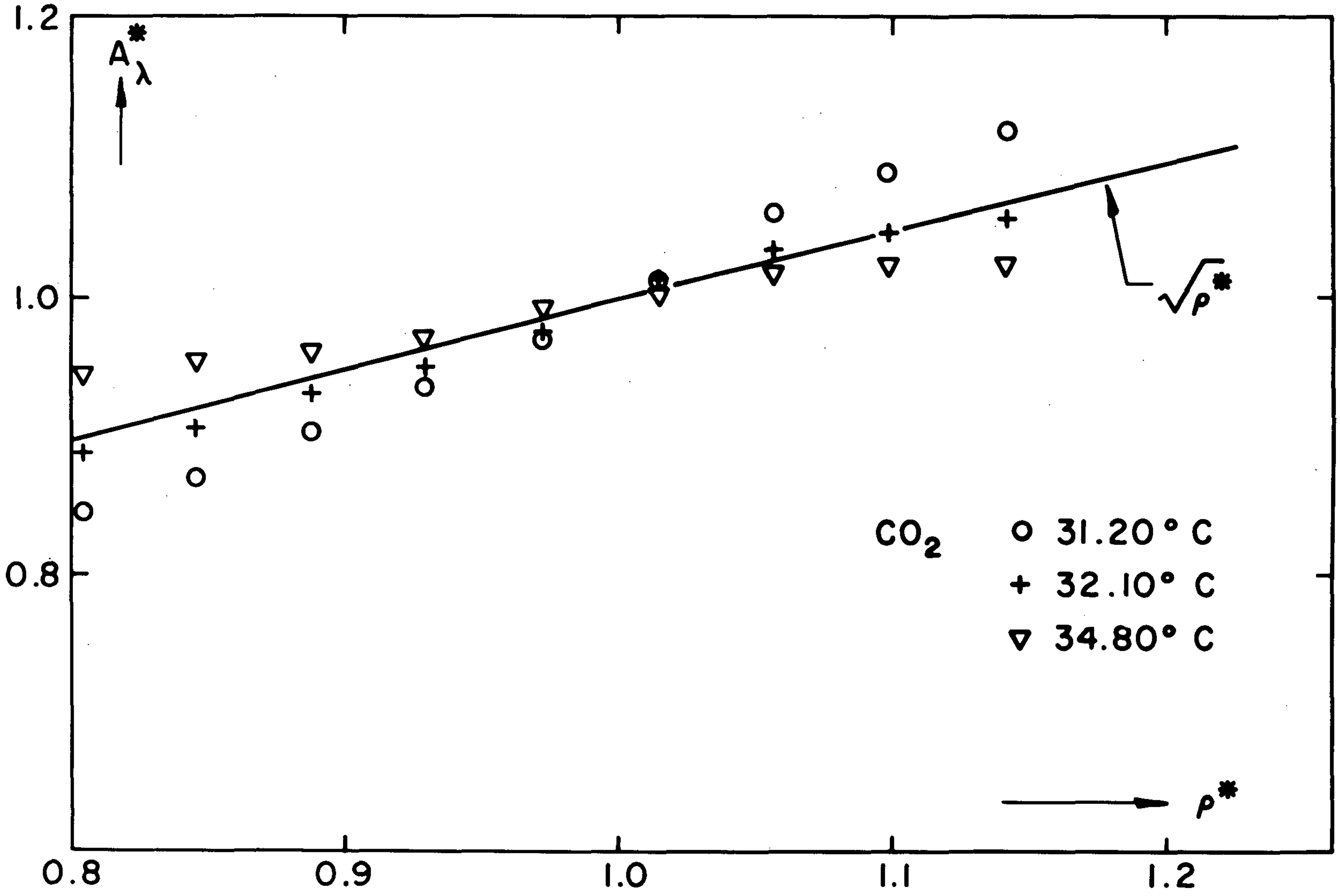

Figure 13. The asymmetry factor $A_\lambda^* = A_\lambda(\rho)/A_\lambda(\rho_c)$ for $\Delta\lambda$ as predicted by the mode-mode coupling theory. $A_\lambda(\rho) \cong \rho^{3/2}\eta/(\partial P/\partial T)_\rho^2$.

data for ξ of CO_2 deduced from X-ray scattering data [C1]. These data can be represented within their experimental precision by (34) with $R = (4.0 \pm 0.2)$ Å, as shown in Fig. 14. In Table V experimental values are presented for the quantity

$$\frac{\Delta\lambda}{\rho(c_p - c_v)} \cdot \frac{6\pi\eta\xi}{k_B T}$$

using $R = 4.0$ Å. This quantity should be equal to unity according to the simple prediction of the mode-mode coupling theory. Of course, in preparing this table we introduce some additional uncertainties, since we are intercomparing results from four experiments [C1,K5,M5,M9]. Nevertheless, the results turn out to be surprisingly close to unity. The irregularities at $\Delta T = 0.2^{\circ}C$ are obviously connected with the fact that the data in the wings of the peak in Fig. 10 are excessively sensitive to small errors in the density. The mode-mode coupling theory appears to reproduce the experimental data to within 15% which is about as good as one can expect from this theory.

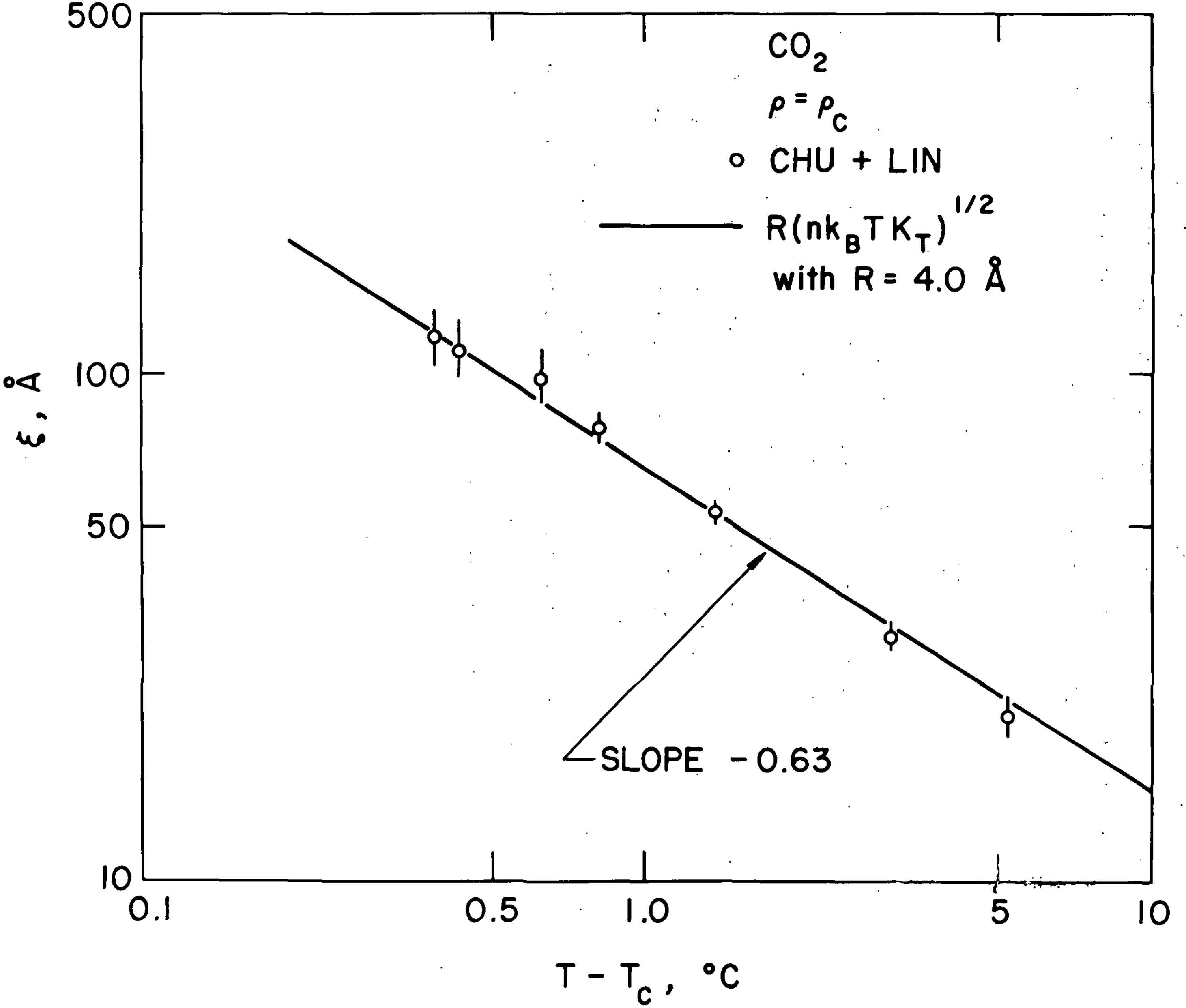

Figure 14. Log-log plot of ξ at $\rho = \rho_c$ as a function of $T-T_c$ for CO_2. The experimental data are those reported by Chu and Lin [C2].

Table V

Comparison of the Experimental Data for CO_2 with the Mode-Mode Coupling Theory*

	$\frac{\Delta\lambda}{\rho(c_p - c_v)} \cdot \frac{6\pi\eta\xi}{k_B T}$			
$T-T_c$ / ρ Amagat	$0.20^{\circ}C$	$1.10^{\circ}C$	$3.\ 0^{\circ}C$	$9.00^{\circ}C$
170	1.16	1.14	1.18	1.15
190	1.00	1.10	1.19	1.14
200	0.97	1.11	1.20	1.14
210	0.98	1.13	1.17	1.13
220	1.10	1.13	1.14	1.10
230	1.17	1.13	1.12	1.08
240	1.22	1.12	1.09	1.06
250	1.34	1.10	1.08	1.03
260	1.17	1.06	1.05	1.00
270	1.02	1.04	1.03	0.96
290	1.03	1.01	0.98	0.88
310	0.93	0.92	0.88	0.78

*ρ_c = 237 amagat.

SECTION IV

DECAY RATE OF FLUCTUATIONS

1. Thermal Diffusivity Near the Gas-Liquid Critical Point

The decay rate of the entropy fluctuations near the gas-liquid critical point is determined by the thermal diffusivity $\chi = \lambda/\rho c_p$ as mentioned in (2). The thermal diffusivity of CO_2 is shown in Fig. 15. These plots are obtained when our thermal conductivity data are divided by calculated values of c_p. These values were obtained by adding experimental c_v data [F6,M11] to the values of c_p-c_v deduced from the compressibility isotherms [M9], as discussed in the previous section.

The decay rate can also be measured directly as the line width of the central component in the spectrum of scattered light [B6,C2,C3,M12,M13]. This method has the advantage that the system remains macroscopically in equilibrium during the experiment. As a result convection can be excluded rigorously and it is possible to approach the critical point considerably more closely than in the thermodynamic experiments discussed above. On the other hand, light scattering experiments become less accurate at a distance away from the critical point, since the intensity of the scattered light decreases rapidly away from the critical point. In practice, therefore, the two methods yield complementary information.

Line width measurements near the gas-liquid critical point have been reported for carbon dioxide [M14,S16], xenon [H5,S17] and sulfur hexafluoride [B7,B8,B9,F7,L7,M15].

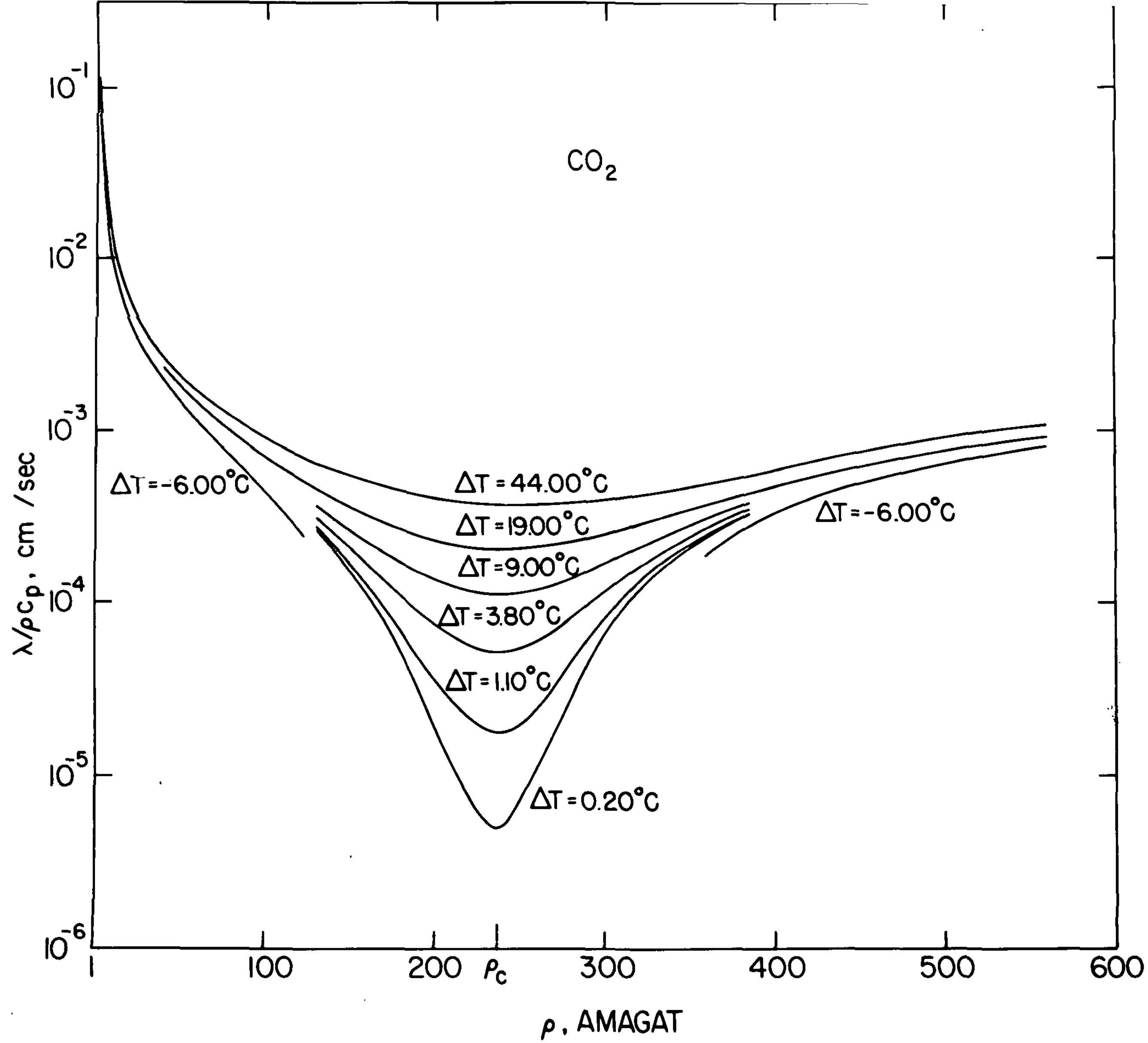

Figure 15. The thermal diffusivity $\lambda/\rho c_p$ of CO_2 as a function of density at various temperatures.

Most of the work thus far reported has been restricted to the temperature dependence of the line width along the critical isochore and the coexistence curve.

Values for the thermal diffusivity of CO_2 at $\rho=\rho_c$ and $T > T_c$, obtained by Swinney and Cummins from light scattering experiments [S16] are represented by the circles in Fig. 16. The squares in this figure represent the thermodynamic data from Fig. 15. It appears that the two sets of data are in satisfactory agreement. The line width measurements of Maccabee and White are also in agreement with these results [M14,W3].

The line width will vanish as $\epsilon^{\gamma-\psi}$ where ψ is the exponent in the power law (30) for the thermal conductivity. According to the mode-mode coupling theory $\gamma-\psi$ should be equal to the exponent ν for the correlation length. This prediction was in apparent disagreement with the values $\gamma-\psi = 0.73 \pm 0.02$ and 0.751 ± 0.004 originally reported for CO_2 and Xe, respectively [H5]. However, as pointed out in a previous paper [S14], the line width measurements should be corrected for the non-singular background term in the thermal conductivity. We thus consider

$$\frac{\Delta\lambda}{\rho(c_p-c_v)} = \chi \cdot \frac{\Delta\lambda}{\lambda} \cdot \frac{c_p}{c_p-c_v} \tag{46}$$

or

$$\frac{\Delta\lambda}{\rho(c_p-c_v)} = \left(\chi - \frac{\lambda_{id}}{\rho c_p}\right) \frac{c_p}{c_p-c_v} \tag{47}$$

where χ is the thermal diffusivity as given by the line width measurements. For completeness, I have also subtracted a background c_v from c_p; this correction, however,

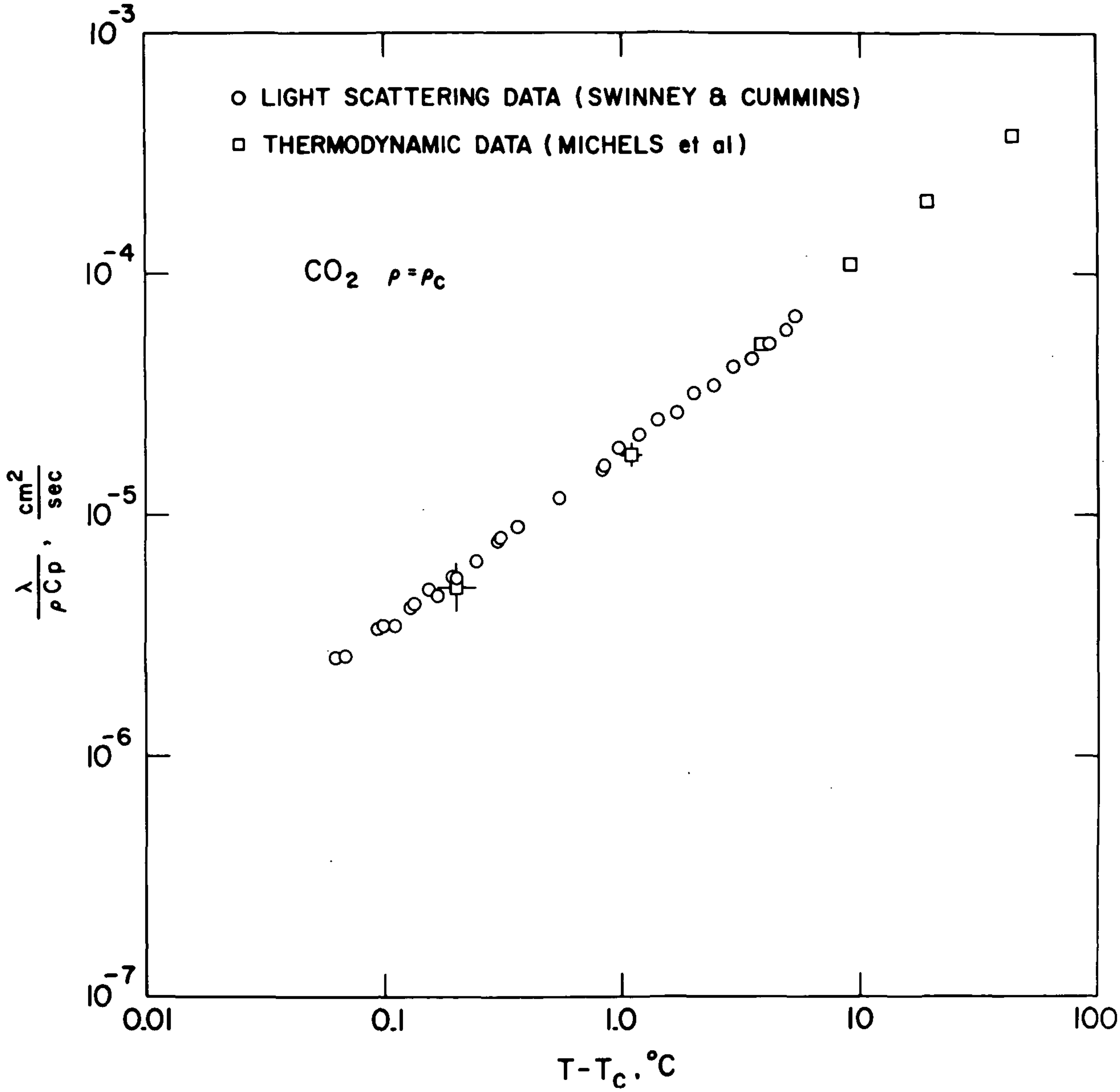

Figure 16. The thermal diffusivity of CO_2 at $\rho = \rho_c$ as a function of temperature. The circles represent the light scattering data of Swinney and Cummins [S15] and the squares represent the thermodynamic data discussed in this report.

is unimportant at the temperatures where the light scattering data were obtained. Both equations (46) and (47) lead to the same results, when applied to the light scattering data of Swinney and Cummins for CO_2. I have a slight preference for (46), since it enables us to calculate the correction factor from our thermal conductivity data more directly. The singular part of the thermal diffusivity, thus deduced from the light scattering data of Swinney and Cummins, is shown in Fig. 17. The corrected data satisfy a power law $\gamma-\psi = 0.63 \pm 0.02$ in good agreement with the prediction of the mode-mode coupling theory and with the exponent deduced from the thermodynamic data. The experimental data of Tufeu, Le Neindre and Bury [T2] enable us to estimate the background contribution λ_{id} to the thermal conductivity of xenon as

$$\lambda_{id} = \lambda_0 + \lambda_1\rho + \lambda_2\rho^2 + \lambda_3\rho^3 + \lambda_4\rho^4 \tag{48}$$

with $\lambda_1 = 5.909 \times 10^{-6}$ $\lambda_2 = 3.817 \times 10^{-9}$

$\lambda_3 = -1.070 \times 10^{-12}$ $\lambda_4 = 0.5904 \times 10^{-15}$

where λ is expressed in W/m^oC and ρ in kg/m^3. Using this estimate, Swinney and coworkers [S17] have recently shown that the exponent $\gamma-\psi$ observed for xenon changes from the uncorrected value 0.75 to a corrected value of 0.64 ± 0.02.

Strictly speaking, the values thus deduced for the exponent $\gamma-\psi$ may only be identified theoretically with the exponent ν of the correlation length, if the temperature dependence of the parameter $\bar{\eta}$ in (40) can be neglected. At the temperatures, where the light scattering measurements were made, the anomalous contribution to the viscosity may not be completely negligible. If we multiply the line

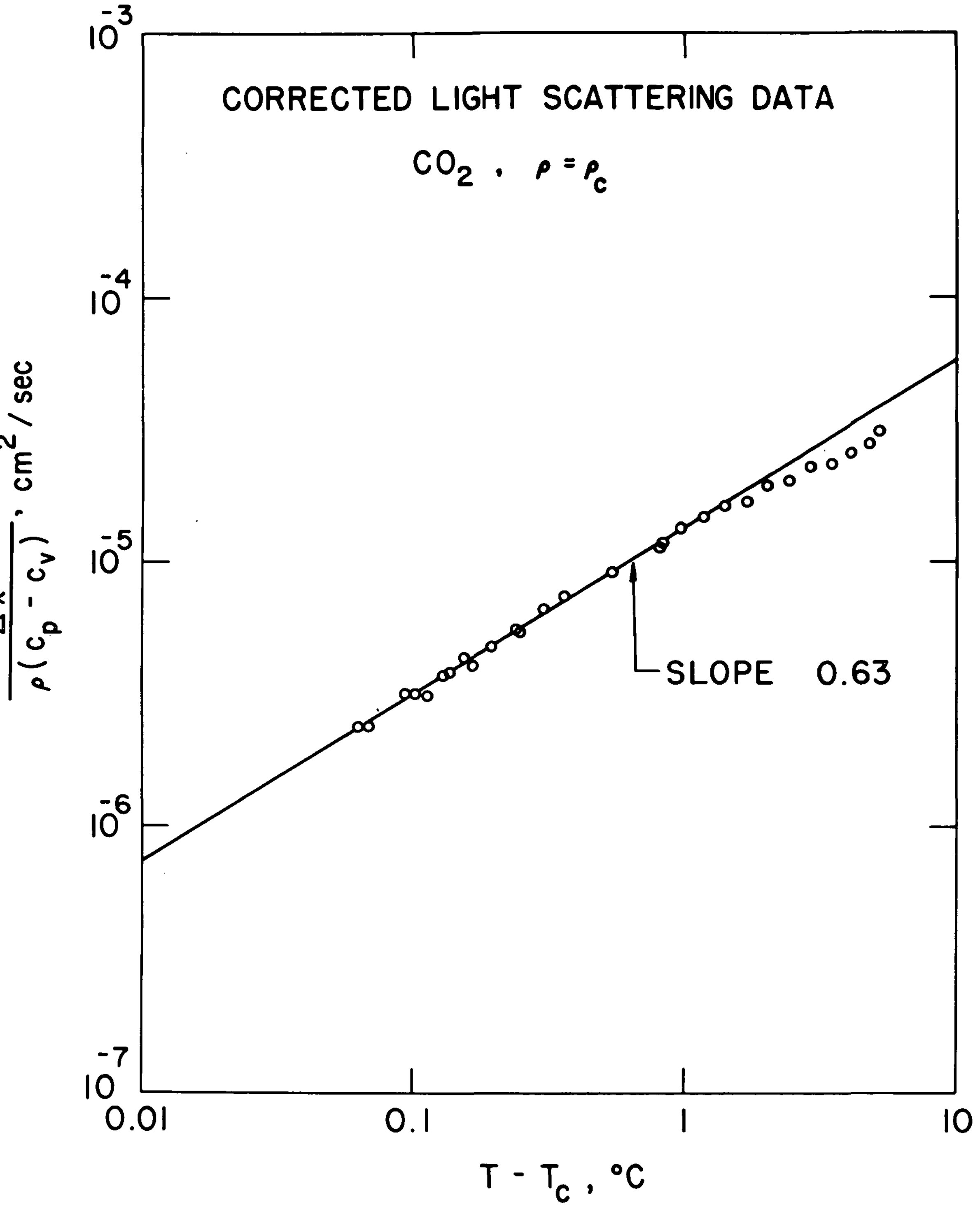

Figure 17. Corrected thermal diffusivities of CO_2 as deduced from the light scattering data of Swinney and Cummins.

width data of Swinney and Cummins for CO_2 with the hydrodynamic viscosity η, estimated by extrapolating the data of Kestin et al. as a function of temperature, and then determine the exponent $\gamma-\psi$, we see that its value reduces even further from 0.63 to 0.61.

The temperature dependence of the thermal diffusivity of SF_6 has been the subject of some controversy since Benedek and coworkers [B7] originally reported an exponent $\gamma-\psi = 1.26$. This value would imply a non-divergent or weakly divergent thermal conductivity, in contrast to what one would conclude from the thermal conductivity measurements of Lis and Kellard [L3,S2]. Subsequent redeterminations of this exponent by various investigators have yielded significantly lower values of this exponent [B8,B9,M15]. The most recent data show that, after correcting for background effects, the value of this exponent for SF_6 is the same as that observed for other gases [F7,L7].

2. Diffusion Near the Critical Mixing Point of Binary Liquids

Thermodynamic measurements of the diffusion coefficient in liquid mixtures did show that the binary diffusion coefficient vanishes at the critical point [C4,H6,K10,K11,L8]. However, with the traditional thermodynamic methods it is difficult to measure the diffusion coefficient very close to the critical point with adequate precision. Nevertheless, the data of Claesson and Sundelöf [C4] and, to a lesser extent, the data of Haase and Siry [H6] for n-hexane-nitrobenzene do indicate that the temperature derivative $(\partial D/\partial T)_c$ tends to become infinite when the critical point is approached. This observation implies that the exponent $\gamma-\psi$ in the power law

$$D \propto \epsilon^{\gamma-\psi} \tag{49}$$

is smaller than one. Therefore, one could have suspected already from the data of Claesson and Sundelöf [C4] that the Onsager coefficient L in (7) diverges, since even in the Van der Waals theory $(\partial\mu/\partial c)_{T,P}$ cannot vanish with an exponent smaller than one. For some reason, however, this conclusion was not drawn by the original investigators [H1,H6,S18].

All current more detailed information concerning the temperature dependence of the diffusion coefficient near the critical mixing point has been obtained from measurements of the decay rate of the concentration fluctuations with light scattering [M16,M17]. Such measurements have been reported for isobutyric-acid-water by Chu and coworkers [C5], for n-hexane-nitrobenzene by Chen and Polonsky-Ostrowsky [C6], for phenol-water by Goldburg et al. [B10,P2], for cyclohexane-aniline and isooctane-perfluoroheptane by Bergé and coworkers [B11,B12,D7,V3]. Measurements of the decay rate of the concentration fluctuations in 3-methylpentane-nitroethane have recently been obtained in our laboratory [C7].

The data have been customarily fitted to a power law (49). A survey of the values reported for the exponent $\gamma-\psi$ at $T > T_c$ is presented in Table VI. For the gas-liquid phase transition it was essential that the decay rate be corrected for a non-singular background term in the thermal conductivity. There is, of course, a priori no reason to expect that a similar background effect would not be present in the decay rate of the concentration fluctuations. In analogy to the gas-liquid phase transition this effect would be determined by the ideal contribution to the Onsager coefficient L in (7). Just as for the gases such a correction would decrease the value of

Table VI

Survey of Diffusivity Measurements

Authors	System	$\gamma-\psi$ (*)	$\gamma-\psi$ (**)
Swinney et al. [S16]	Carbon Dioxide	0.73 ± 0.02	0.63 ± 0.02
Swinney et al. [H5,S17]	Xenon	0.75 ± 0.004	0.64 ± 0.02
Lim et al. [L7] Feke et al. [F7]	Sulfur hexafluoride	$0.78 \pm$?	0.61 ± 0.04
Chu et al. [C5]	Isobutyric acid-water	0.68 ± 0.04	?
Chen et al. [C6]	n-hexane-nitrobenzene	0.66 ± 0.02	?
Pusey et al. [P2]	Phenol-water	0.68 ± 0.03	?
Bergé et al. [B12]	Aniline-cyclohexane	0.61 ± 0.07	?
Chang et al. [C7]	3-methylpentane-nitroethane	0.67 ± 0.02	0.62 ± 0.02

(*) Uncorrected.

(**) Corrected.

the exponent $\gamma-\psi$. Furthermore, the assumption that $\overline{\eta}$ in (41) is independent of temperature is also not justified. The existence of a viscosity anomaly has been well documented and the anomalous contribution to the hydrodynamic viscosity is not negligible at the temperature where most light scattering experiments have been obtained. If one assumes that the temperature dependence of $\overline{\eta}$ is equal to that of the experimental hydrodynamic viscosity, one finds a correction which also reduces the value of the exponent $\gamma-\psi$. The latter point was also made by Bergé and Dubois [B13]. Further research is needed to make a quantitative assessment of the corrections due to background effects and to the anomalous temperature dependence of the viscosity.

SECTION V

CONCLUSIONS

The shear viscosity of binary liquids exhibits an anomalous temperature dependence near the critical mixing point which is close to logarithmic. Existing experimental data do not enable us to discriminate between a weak power law divergence or a cusp-like behavior. The existence of a weak anomaly in the viscosity of gases near the gas-liquid critical point appears probable, but has not yet been demonstrated conclusively.

In order to deduce the asymptotic behavior of the transport properties, it is essential that all transport properties be corrected for non-singular background contributions.

The anomalous thermal conductivity near the gas-liquid critical point satisfies scaling law relations similar to those previously established for equilibrium properties. It appears that the thermal conductivity anomaly can be to a good approximation related to the *equilibrium* correlation length.

The mode-mode coupling theory for the dynamical slowing down of the fluctuations is in substantial agreement with experiment at those temperatures, where the anomalous contribution to the viscosity is negligibly small.

REFERENCES

A1. G. Arcovito, C. Faloci, M. Roberti and L. Mistura, Phys. Rev. Letters 22, 1040 (1969).

A2. J. C. Allegra, A. Stein and G. F. Allen, J. Chem. Phys. 55, 1716 (1971).

A3. Kh. I. Amirkhanov and A. P. Adamov, Teploenergetika 10, no. 7, 77 (1963); Primenenie Ultraakustiki k Issledovan Vesch. 18, 65 (1963).

B1. J. Brunet and K. E. Gubbins, Trans. Faraday Soc. 65, 1255 (1969).

B2. T. R. Barber and J. V. Champion, Physics Letters 29A, 622 (1969).

B3. B. J. Bailey and K. Kellner, Brit. J. Appl. Phys. 18, 1645 (1967); Physica 39, 444 (1968).

B4. R. S. Brokaw and R. A. Svehla, J. Chem. Phys. 44, 4643 (1966).

B5. R. S. Brokaw, "Statistical mechanical theories of transport properties," NASA TM X-52478 (NASA, Washington, D. C., 1968).

B6. G. B. Benedek in "Statistical Physics. Phase Transformations and Superfluidity," M. Chrétien, E. P. Gross and S. Deser, eds. (Gordon and Breach, New York, 1968), Vol. 2, p. 1.

B7. G. B. Benedek, in "Polarisation Matière et Rayonnement" (Presses Universitaires de France, Paris, 1969), p. 49.

B8. G. B. Benedek, J. B. Lastovka, M. Giglio and D. Cannell in "Critical Phenomena in Alloys, Magnets and Superconductors," R. E. Mills, E. Ascher and R. I. Jaffee, eds. (McGraw-Hill, New York, 1971), p. 503.

B9. P. Braun, D. Hammer, W. Tscharnuter and P. Weinzierl, Phys. Letters 32A, 390 (1970).

B10. C. S. Bak and W. I. Goldburg, Phys. Rev. Letters 23, 1218 (1969).

B11. P. Bergé, P. Calmettes, C. Laj and B. Volochine, Phys. Rev. Letters 23, 693 (1969).

B12. P. Bergé, P. Calmettes, C. Laj, M. Tournarie and B. Volochine, Phys. Rev. Letters 24, 1223 (1970).

B13. P. Bergé and M. Dubois, Phys. Rev. Lett. 27, 1124 (1971).

C1. B. Chu and J. S. Lin, J. Chem. Phys. 53, 4454 (1970).

C2. B. Chu, Ann. Rev. Phys. Chem. 21, 145 (1970).

C3. H. Z. Cummins and H. L. Swinney, in "Progress in Optics," E. Wolf, ed. (North Holland Publ. Co., Amsterdam, 1970), Vol. 8, Ch. 3.

C4. S. Claesson and L. O. Sundelöf, J. Chim. physique 54, 914 (1957).

C5. B. Chu, F. J. Schoenes and M. E. Fisher, Phys. Rev. 185, 219 (1969).

C6. S. H. Chen and N. Polonsky-Ostrowsky, Optics Comm. 1, 64 (1969); J. Phys. Soc. Japan 26, Suppl., 179 (1969).

C7. R. F. Chang, P. H. Keyes, J. V. Sengers and C. O. Alley, Phys. Rev. Lett. 27, 1706 (1971).

D1. S. R. De Groot and P. Mazur, "Non-Equilibrium Thermodynamics" (North-Holland Publ. Co., Amsterdam, 1962).

D2. P. Debye, Phys. Rev. Letters 14, 783 (1965).

D3. P. Drapier, Bull. Acad. Belg. Cl. Soc., p. 621 (1911).

D4. P. Debye, B. Chu and D. Woermann, J. Polymer Science A1, 249 (1963).

D5. J. M. Deutsch and R. Zwanzig, J. Chem. Phys. 46, 1612 (1967).

D6. D. E. Diller, J. Chem. Phys. 42, 2089 (1965).

D7. M. Dubois and P. Bergé, Phys. Lett. 37A, 155 (1971).

F1. J. Friedländer, Z. physik.Chem. 38, 385 (1901).

F2. M. Fixman, J. Chem. Phys. 36, 310 (1962).

F3. M. Fixman, J. Chem. Phys. 47, 2808 (1967); Discussions Faraday Soc. 43, 70 (1967).

F4. R. A. Ferrell, N. Menyhàrd, H. Schmidt, F. Schwabl and P. Szépfalusy, Annals of Physics 47, 565 (1968).

F5. M. E. Fisher, J. Math. Phys. 5, 944 (1964).

F6. K. Fritsch and E. F. Carome, "Behavior of fluids in the vicinity of the critical point," NASA CR-1670 (NASA, Washington, D. C., 1970).

F7. G. T. Feke, G. A. Hawkins, J. B. Lastovka and G. B. Benedek, Phys. Rev. Lett. 27, 1780 (1971).

G1. L. I. Gvozdeva and A. P. Lyubimov, Izv. Vysshikn. Uchetn. Zavedenii, Chem. Met. 8, 16 (1965).

G2. E. Gulari, A. F. Collings, R. L. Schmidt and C. J. Pings, J. Chem. Phys. 56 (1972).

G3. R. B. Griffiths and J. C. Wheeler, Phys. Rev. A2, 1047 (1970).

G4. L. A. Guildner, Proc. Nat. Acad. Sci. U.S.A. 44, 1149 (1958); J. Res. NBS 66A, 333, 341 (1962).

G5. I. F. Golubev and V. P. Sokolova, Teploenergetika 11, no. 9, 64 (1964).

G6. R. B. Griffiths, Phys. Rev. 158, 176 (1967).

H1. R. Haase, "Thermodynamics of Irreversible Processes" (Addison-Wesley, Reading, Mass., 1969).

H2. B. I. Halperin and P. C. Hohenberg, Phys. Rev. 177, 952 (1969).

H3. W. Herreman, A. Lattenist, W. Grevendonk and A. De Bock, Physics 52, 489 (1971).

H4. R. C. Hendricks and A. Baron, Paper 71-HT-28 (Heat Transfer Division, ASME, New York, 1971).

H5. D. L. Henry, H. L. Swinney and H. Z. Cummins, Phys. Rev. Letters 25, 1170 (1970).

H6. R. Haase and M. Siry, Z. physik. Chem. Neue Folge 57, 56 (1968).

I1. L. D. Ikenberry and S. A. Rice, J. Chem. Phys. 39, 1561 (1963).

K1. N. E. Khazanova and L. R. Linshits, Doklady Akad. Nauk SSSR 84, 1191 (1952).

K2. L. P. Kadanoff and J. Swift, Phys. Rev. 166, 89 (1968).

K3. K. Kawasaki, Annals of Physics 61, 1 (1970).

K4. K. Kawasaki in "Critical Phenomena in Alloys, Magnets and Superconductors," R. E. Mills, E. Ascher and R. I. Jaffee, eds. (McGraw-Hill, New York, 1971), p. 489.

K5. J. Kestin, J. H. Whitelaw and T. F. Zien, Physica 30, 161 (1964).

K6. J. F. Kerrisk and W. E. Keller, Phys. Rev. 177, 341 (1969).

K7. L. P. Kadanoff, Physics 2, 263 (1966).

K8. J. T. Kennedy and G. Thodos, A.I.Ch.E. Journal 7, 625 (1961).

K9. L. P. Kadanoff, "Varenna Lectures on Critical Phenomena," M. S. Green, ed. (Academic Press, New York).

K10. I. R. Krichevskii, N. E. Khazanova and L. R. Linshits, Dokl. Akad. Nauk. SSSR 99, 113 (1954).

K11. I. R. Krichevskii, N. E. Khazanova and I. V. Tsekhanskaia, Russ. J. Phys. Chem. 34, 598 (1960).

L1. L. D. Landau and E. M. Lifshitz, "Statistical Physics" (Addison-Wesley, Reading, Mass., 1958).

L2. H. M. Leister, J. C. Allegra and G. F. Allen, J. Chem. Phys. 51, 3701 (1969).

L3. J. Lis and P. O. Kellard, Brit. J. Appl. Phys. 16, 1099 (1965).

L4. B. Le Neindre, P. Bury, R. Tufeu, P. Johannin and B. Vodar, Proc. 9th Thermal Conductivity Conference, H. R. Shanks, ed. (USAEC Division of Technical Information, Oak Ridge, Tenn., 1970), p. 69.

L5. J. H. Lunacek and D. S. Cannell, Phys. Rev. Letters 27, 841 (1971).

L6. L. D. Landau and E. M. Lifshitz, "Fluid Mechanics" (Addison-Wesley, Reading, Mass., 1958).

L7. T. K. Lim, H. L. Swinney, K. H. Langley and Th. A. Kachnowski, Phys. Rev. Letters 27, 1776 (1971).

L8. H. L. Lorentzen and B. B. Hansen, Acta Chem. Scand. 11, 893 (1957); 12, 139 (1958).

M1. L. Mistura and C. Cohen, Phys. Rev. A4, 253 (1971).

M2. R. D. Mountain and R. Zwanzig, J. Chem. Phys. 48, 1451 (1968).

M3. A. Michels, A. Botzen and W. Schuurman, Physica 23, 95 (1957).

M4. A. Michels and J. V. Sengers, Physica 28, 1238 (1962).

M5. A. Michels, J. V. Sengers and P. S. Van der Gulik, Physica 28, 1201, 1216 (1962).

M6. M. L. R. Murthy and H. A. Simon, Phys. Rev. A2, 1458 (1970); Proc. 5th Symposium on Thermophysical Properties, C. F. Bonilla, ed. (ASME, New York, 1970), p. 214.

M7. M. Vicentini-Missoni, J. M. H. Levelt Sengers and M. S. Green, J. Res. NBS 73A, 563 (1969); Phys. Rev. Letters 22, 389 (1969).

M8. M. Vicentini-Missoni, R. I. Joseph, M. S. Green and J. M. H. Levelt Sengers, Phys. Rev. B1, 2312 (1970).

M9. A. Michels, B. Blaisse and C. Michels, Proc. Roy. Soc. (London) A160, 358 (1937).

M10. A. Münster, in "Fluctuation Phenomena in Solids," R. E. Burgess, ed. (Academic Press, New York, 1965), Ch. 6.

M11. A. Michels and J. C. Stryland, Physica 18, 613 (1952).

M12. R. D. Mountain, Rev. Mod. Phys. 38, 205 (1966).

M13. D. McIntyre and J. V. Sengers, in "Physics of Simple Liquids," H. N. V. Temperley, J. S. Rowlinson and G. S. Rushbrooke, eds. (North Holland Publ. Co., Amsterdam, 1968), Ch. 11.

M14. B. S. Maccabee and J. A. White, Phys. Rev. Letters 27, 495 (1971).

M15. R. Mohr and K. H. Langley, Journal de Physique (1972).

M16. R. D. Mountain, J. Res. NBS 69A, 523 (1965).

M17. R. D. Mountain and J. M. Deutch, J. Chem. Phys. 50, 1103 (1969).

N1. S. N. Naldrett and O. Maass, Can. J. Research 18B, 322 (1940).

N2. D. P. Needham and H. Ziebland, Int. J. Heat Mass Transfer 8, 1307 (1965).

P1. I. Prigogine, ed., "Transport Processes in Statistical Mechanics" (Interscience, New York, 1958), pp. 382, 394, 395.

P2. P. N. Pusey and W. I. Goldburg, Phys. Rev. Letters 23, 67 (1969); Phys. Rev. A3, 766 (1971).

R1. T. M. Reed and T. E. Taylor, J. Phys. Chem. 63, 58 (1959).

R2. H. M. Roder and D. E. Diller, J. Chem. Phys. 52, 5928 (1970).

S1. J. V. Sengers, NBS Misc. Publ. 273, M. S. Green and J. V. Sengers, eds. (U. S. Govt. Printing Office, Washington, D. C., 1966), p. 165.

S2. J. V. Sengers, "Varenna Lectures on Critical Phenomena," M. S. Green, ed. (Academic Press, New York, 1972).

S3. O. Scarpa, Nuovo Cimento (5)6, 277 (1903); J. Chim. Phys. 2, 447 (1904).

S4. V. K. Semenchenko and E. L. Zorina, Doklady Akad. Nauk SSSR 73, 331 (1950); 80, 903 (1951); 84, 1191 (1952); Zh. Fiz. Khim. 26, 520 (1952).

S5. A. Stein, J. C. Allegra and G. F. Allen, J. Chem. Phys. 55, 4265 (1971).

S6. A. Stein, J. Davidson, J. C. Allegra and G. F. Allen, J. Chem. Phys. 56 (1972).

S7. R. Sallavanti and M. Fixman, J. Chem. Phys. 48, 5326 (1968).

S8. J. Swift, Phys. Rev. 173, 257 (1968).

S9. J. V. Sengers, Int. J. Heat Mass Transfer 8, 1103 (1965).

S10. J. V. Sengers and A. Michels, Proc. 2nd Symposium on Thermophysical Properties, J. F. Masi and D. H. Tsai, eds. (ASME, New York, 1962), p. 434.

S11. H. A. Simon and E. R. G. Eckert, Int. J. Heat Mass Transfer 6, 681 (1963).

S12. V. P. Sokolova and I. F. Golubev, Teploenergetika 14, no. 4, 91 (1967).

S13. J. M. H. Levelt Sengers, Ind. Eng. Chem. Fundam. 9, 470 (1970).

S14. J. V. Sengers and P. H. Keyes, Phys. Rev. Letters 26, 70 (1971).

S15. J. V. Sengers, Recent Advances in Engineering Science, Vol. III, A. C. Eringen, ed. (Gordon and Breach, New York, 1968), p. 153.

S16. H. L. Swinney and H. Z. Cummins, Phys. Rev. 171, 152 (1968).

S17. H. L. Swinney, D. L. Henry and H. Z. Cummins, Journal de Physique (1972).

S18. L. O. Sundelöf, Arkiv Kemi 15, 317 (1960).

T1. B. C. Tsai, Master's thesis, Univ. Akron, 1970.

T2. R. Tufeu, B. Le Neindre and P. Bury, Comptes rendus 273B, 113 (1971).

V1. L. Van Hove, Phys. Rev. 95, 1374 (1954).

V2. M. P. Vukalovich and V. V. Altunin, "Thermophysical Properties of CO_2" (Collet's Publ. London, 1968).

V3. B. Volochine, P. Bergé and I. Lagues, Phys. Rev. Letters 25, 1414 (1970).

W1. D. Woermann and W. Sarholz, Ber. Bunsenges. physik. Chem. 69, 319 (1965).

W2. B. Widom, J. Chem. Phys. 43, 3898 (1965).

W3. J. A. White and B. S. Maccabee, Phys. Rev. Letters 26, 1468 (1971).

Z1. E. F. Zhuralev, Zh. obschch. Khim. 31, 363 (1961).

Z2. H. Ziebland and J. T. A. Burton, Brit. J. Appl. Phys. 9, 52 (1958).

Z3. R. Zwanzig, "Nonlinear Dynamics of Collective Modes," Technical Note BN-695, Institute for Fluid Dynamics and Applied Mathematics, University of Maryland, College Park, Md. (1971).

NASA-Langley, 1972 —— 33 E-6980